Detection and functional resolution of soluble multimeric immune complexes by a comprehensive FcγR reporter cell panel

Haizhang Chen[1,2], Andrea Maul-Pavicic[3,4], Martin Holzer[5], Magdalena Huber[1,2], Ulrich Salzer[3], Nina Chevalier[3], Reinhard E. Voll[3,4], Hartmut Hengel[1,2,*] & Philipp Kolb[1,2,*]

[1]Institute of Virology, University Medical Center, Albert-Ludwigs-University Freiburg, Hermann-Herder-Str. 11, 79104 Freiburg, Germany

[2]Faculty of Medicine, Albert-Ludwigs-University Freiburg, 79104 Freiburg, Germany

[3]Department of Rheumatology and Clinical Immunology, Medical Center - University of Freiburg, Faculty of Medicine, University of Freiburg, Hugstetterstr. 55, 79106 Freiburg, Germany

[4]Center for Chronic Immunodeficiency (CCI), Medical Center-University of Freiburg, Faculty of Medicine, University of Freiburg, Breisacherstr. 115, 79106 Freiburg, Germany

[5]Institute for Pharmaceutical Sciences, Albert-Ludwigs-University Freiburg, Hermann-Herder-Str. 9, 79104 Freiburg, Germany

*corresponding authors (Hartmut.hengel@uniklinik-freiburg.de)

One Sentence Summary: In this study we established a comprehensive FcγR reporter cell assay enabling the detection and quantification of soluble immune complexes generated in experimental and clinical settings.

Abstract: Fc-gamma receptor (FcγR) activation by soluble IgG immune complexes (sICs) represents a major mechanism of inflammation in certain autoimmune diseases such as systemic lupus erythematosus (SLE). A robust and scalable test system allowing for the detection and quantification of sIC bioactivity is missing. Previously described FcγR interaction assays are limited to certain FcγRs, lack scalability and flexibility, are not indicative of receptor activation or lack sensitivity towards sIC size. We developed a comprehensive reporter cell panel detecting individual activation of FcγRs from humans and the mouse. The reporter cell lines were integrated into an assay format that provides flexible read-outs enabling the quantification of sIC reactivity via ELISA or a fast detection using flow cytometry. This identified FcγRIIA(H) and FcγRIIIA as the most sIC-sensitive FcγRs in our test system. Applying the assay we demonstrate that sICs versus immobilized ICs are fundamentally different FcγR-ligands with regard to FcγR preference and signal strength. Reaching a detection limit in the very low nanomolar range, the assay proved also to be sensitive to sIC stoichiometry and size enabling for the first time a complete reproduction of the Heidelberger-Kendall precipitation curve in terms of immune receptor activation. Analyzing sera from SLE patients and mouse models of lupus and arthritis proved that sIC-dependent FcγR activation has predictive capabilities regarding severity of SLE disease. The new methodology provides a sensitive, scalable and comprehensive tool to evaluate the size, amount and bioactivity of sICs in all settings.

Introduction

Immunoglobulin G (IgG) is the dominant immunoglobulin isotype in chronic infections and in various antibody-mediated autoimmune diseases. The multi-faceted effects of the IgG molecule rely both on the F(ab) regions, which recognize a specific antigenic determinant to form immune complexes (ICs), and the constant Fc region (Fcγ), which is detected by effector molecules like the Fcγ receptors (FcγRs) found on most cells of the immune system or C1q of

the complement system. When IgG binds to its antigen ICs are formed, which, depending on the respective antigen, are either matrix/cell-bound or soluble (sICs). The composition of sICs is dependent on the number of epitopes recognized by IgG on a single antigen molecule and the ability of the antigen to form multimers. Fcγ-FcγR binding is necessary but not sufficient to activate FcγRs since physical receptor cross-linking is required for receptor triggering (Duchemin et al, 1994; Luo et al, 2010; Patel et al, 2019). IgG opsonized infected cells or microorganisms are readily able to cross-link FcγRs (Bruhns et al, 2009; Lux et al, 2013). This initiates various signalling pathways (Greenberg et al, 1994; Kiefer et al, 1998; Luo et al, 2010) which in turn regulate immune cell effector functions (Bournazos et al, 2017; Nimmerjahn & Ravetch, 2010). It is also suggested that sICs can dynamically tune FcγR triggering, implying that changes in sIC size directly impact strength and duration of FcγR responses (Lux et al, 2013). However, the molecular requirements are largely unknown and a translation to bioactivity of the paradigmatic Heidelberger-Kendall precipitation curve, describing that sIC size depends on the antigen:antibody ratio, is so far missing (Heidelberger & Kendall, 1929; Heidelberger & Kendall, 1935).

Among all type I FcγRs, FcγRIIB (CD32B) is the only inhibitory receptor, signalling via immunoreceptor tyrosine-based inhibitory motifs (ITIMs), while the activating receptors are associated with immunoreceptor tyrosine-based activation motifs (ITAMs). Another exception is FcγRIIIB (CD16B), which is glycosylphosphatidylinositol (GPI)-anchored and lacks a signalling motif (Bruhns, 2012; Bruhns & Jonsson, 2015; Nimmerjahn & Ravetch, 2006; Nimmerjahn & Ravetch, 2008). Still, FcγRIIIB is widely accepted to be a neutrophil activating receptor, e.g. by cooperating with other FcγRs such as FcγRIIA (Vossebeld et al, 1997). FcγRI (CD64) is the only high affinity FcγR binding also to monomeric IgG, while all other FcγRs only efficiently bind to complexed, i.e. antigen-bound IgG (Bruhns, 2012; Bruhns & Jonsson, 2015; Lu et al, 2018). Activation of FcγRs leads to a variety of cellular effector functions elicited by several immune cells such as natural killer (NK) cells via FcγRIIC/FcγRIIIA,

monocyte-derived cells via FcγRI/FcγRIIB/FcγRIIIA, granulocytes via FcγRI/FcγRIIA/FcγRIIIB, platelets via FcγRIIA and B cells via FcγRIIB. Consequently, FcγRs connect and regulate both the innate and adaptive branches of the immune system. Various factors have been shown to influence IC-dependent FcγR activation profiles, including FcγR-Fcγ binding affinity and avidity (Koenderman, 2019), IgG subclass, glycosylation patterns and genetic polymorphism (Bruhns et al, 2009; Pincetic et al, 2014; Plomp et al, 2017; Vidarsson et al, 2014), stoichiometry of antigen-antibody-ratio (Berger et al, 1996; Lux et al, 2013; Pierson et al, 2007) and FcγR clustering patterns (Patel et al, 2019). Specifically, Asn297-linked glycosylation patterns of the IgG Fc domain initiate either pro- or anti-inflammatory effector pathways by tuning the binding affinity to activating versus inhibitory FcγRs, respectively (Bohm et al, 2014). However, despite being explored in proof-of-concept studies, the functional consequences of these ligand features on a given FcγR are still not fully understood. Therefore, there is an obvious need for an assay platform allowing for the systematic assessment of IC-mediated FcγR activation.

sICs and immobilized ICs represent unequal and discrete stimuli for the immune system (Fossati et al, 2002; Granger et al, 2019). Soluble circulating ICs are commonly associated with certain chronic viral or bacterial infections (Wang & Ravetch, 2015; Yamada et al, 2015) and autoimmune diseases, such as systemic lupus erythematosus (SLE) or rheumatoid arthritis (RA) (Antes et al, 1991; Koffler et al, 1971; Zubler et al, 1976). When deposited and accumulating in tissues, sICs can cause local damage due to inflammatory responses, classified as type III hypersensitivity (Rajan, 2003). Compared with immobilized local ICs, which recruit immune cells causing tissue damage (Mayadas et al, 2009; Mulligan et al, 1991; Ward et al, 2016), sIC related disorders are characterized by systemic inflammation which is reflected by immune cell exhaustion and senescence (Bano et al, 2019; Chauhan, 2017; Tahir et al, 2015). In order to resolve sIC-dependent activation of FcγRs in greater detail, we developed a scalable reporter system suited for two high throughput readouts, capable of quantifying and distinguishing the

101 activation of single FcγRs. As the assay is also sensitive to stoichiometry and sIC size, we were
102 able to translate the Heidelberger-Kendall precipitation curve to FcγR bioactivity. Compared to
103 currently available ELISA assays detecting sICs by their affinity to C1q-CIC (circulating
104 immune complexes) or C3d, the assay system presented below is strictly specific for IgG
105 immune complexes and integrates sICs of all sizes into single Fcγ receptor bioactivity.
106 Applying reporter cell lines enables very high sensitivity in the low nanomolar range, as signals
107 are biologically amplified compared to biochemical binding based read-outs. Finally, we
108 applied the assay to a clinical setting, measuring sICs in sera from SLE patients. A reporter cell
109 panel expressing murine FcγRs revealed the detection of sICs in the serum of autoimmune-
110 prone diseased mice in preclinical models of lupus and arthritis. Prospectively, this
111 methodology could be instrumental as an experimental and clinical toolbox to unveil sIC-
112 mediated FcγR activation in various autoimmune or infectious diseases.
113
114 **Results**
115 *Experimental assay setup*
116 The assay used in this study was adapted from a previously described cell-based FcγR activation
117 test system designed to measure receptor activation in response to opsonized virus infected cells
118 (Corrales-Aguilar et al, 2013; Kolb et al, 2021) and therapeutic Fc-fusion proteins (Lagasse et
119 al, 2019). We refined the assay to enable selective detection of sICs and expanded the reporter
120 cell line-up (FcγRI: Acc# LT744984; FcγRIIA (131R): Acc# M28697; FcγRIIA(131H): Acc#
121 XP_011507593; FcγRIIB/C: Acc# LT737639; FcγRIIIA(176V): Acc# LT737365;
122 FcγRIIIB(176V): Acc# O75015). Ectodomains of FcγRIIB and FcγRIIC are identical. Second
123 generation reporter cells were generated to improve stable expression of chimeric FcγRs
124 compared to the transfectants used in the original assay (Corrales-Aguilar et al, 2013). To this
125 end, mouse BW5147 cells were transduced as described previously via lentiviral transduction
126 (Corrales-Aguilar et al, 2013; Halenius et al, 2011; Van den Hoecke et al, 2017). Human FcγR

127 expression on transduced cells after puromycin selection and two consecutive cell sorting steps
128 was assessed by flow cytometry (Fig. 1A). FcγR activation is measured by surface CD69
129 expression after 4h of incubation using high thoughput flow cytometry or by quantification of
130 IL-2 secretion after 16 h of incubation using ELISA. Suspension of IgG or sICs in the liquid
131 phase is enforced by pre-incubation of a 96 well ELISA microtiter plate with PBS/FCS blocking
132 buffer (Fig. 1B). To this end, we compared graded concentrations of FCS in the blocking
133 reagent and measured the threshold at which IgG was no longer adsorbed to the plate and stayed
134 abundantly in solution. FCS supplementation to 1% (v/v) or higher is sufficient to keep IgG
135 antibodies in solution. We then set out to test if immobilized IgG can be used as an operational
136 surrogate for IgG-opsonized cells or immobilized ICs with regard to FcγR activation as
137 suggested previously (Tanaka et al, 2009). We found no qualitative difference in FcγR
138 activation between immobilized Rtx, immobilized ICs (Rtx + rec. CD20) or Rtx-opsonized
139 293T-CD20 cells (Fig. 1C). In contrast, sICs formed by monomeric CD20 antigen (aa 141-188)
140 and Rtx failed to activate FcγRs even at very high ligand concentrations. We concluded that
141 FcγR-crosslinking by sICs is only achieved by multivalent antigens but not dimeric ICs. Of
142 particular note, to reliably and accurately differentiate between strictly soluble and immobilized
143 including aggregated triggers using this assay, reagents for the generation of synthetic ICs
144 needed to be of therapy-grade purity. The assay setup is depicted in Fig. 1D.
145
146 *Detection of human FcγR activation by multimeric sICs*
147 Next, we generated synthetic sICs from recombinant ultrapure molecules to evaluate the assay.
148 We aimed to avoid the use non-human molecules, misfolded IgG aggregates or IgG-IgG
149 complexes to generate a most native and defined ligand. To date, there are still few
150 commercially available human IgG-antigen pairs that meet both the above mentioned high
151 grade purity requirements while also consisting of at least two antigen monomers. In order to
152 meet these stipulations we focused on three pairs of multivalent antigens and their respective

153 mAbs that were available in required amounts enabling large-scale titration experiments;
154 trimeric rhTNFα:IgG1 infliximab (TNFα:Ifx), dimeric rhVEGFA: IgG1 bevacizumab
155 (VEGFA/Bvz) and dimeric rhIL-5: IgG1 mepolizumab (IL-5/Mpz). As lymphocytes express
156 TNFα-receptors I and II while not expressing receptors for IL-5 or VEGFA, we tested whether
157 the mouse lymphocyte derived BW5147 thymoma reporter cell line is sensitive to high
158 concentrations of rhTNFα. Toxicity testing revealed that even high concentrations of up to
159 76.75 nM rhTNFα did not affect viability of reporter cells (Fig. S1). Next, we measured the
160 dose-dependent activation of human FcγRs comparing immobilized IgG to sICs (TNFα:Ifx)
161 using the full FcγR reporter cell panel (Fig. 2). Soluble antigen or mAb alone served as negative
162 controls showing no background activation even at high concentrations. Immobilized rituximab
163 (Rtx, human IgG1) and immobilized FcγR-specific mouse mAbs served as positive controls for
164 inter-experimental reference. All FcγRs were activated by immobilized IgG. Only FcγRI failed
165 to respond when reporter cells were incubated with sICs. Both the IL-2 ELISA as well as the
166 CD69 expression read-out gave comparable results. Further, using an IL-2 standard, we were
167 able to quantify FcγR activation (right y-axis). This revealed that the reporter cell lines differ
168 regarding reactivity which did not correlate with receptor expression. Although the low signals
169 for FcγRI might be linked to receptor expression, responsiveness was markedly lower compared
170 to other reporter cell lines (Fig. 1A). Attempts to increase and equalize receptor expression by
171 repeated cell sorting steps failed, indicating that individual receptors only tolerate limited
172 molecule densities on the reporter cell surfaces.
173
174 *Evaluation of human FcγR activation by multimeric sICs*
175 The assay proved to be sensitive to sICs in the nanomolar range. Regarding immobilized IgG,
176 the detection limit was between 1 to 3 nM. sICs were detected with the following limits
177 regarding the IL-2 readout: FcγRI – no detection; FcγRIIA(R) – 3 nM; FcγRIIA(H) – 0.2 nM;
178 FcγRIIB/C – 3 nM; FcγRIIIA – 0.2 nM; FcγRIIIB - 25 nM. We observed that sICs and

179 immobilized ICs induce largely different signal strength in individual reporter cell lines. FcγRI
180 and FcγRIIIB were more efficiently activated by immobilized IgG compared to sICs.
181 Conversely, FcγRIIA(H) and FcγRIIIA were more efficiently activated by sICs. FcγRIIB/C
182 showed discrepant results when comparing the IL-2 read-out (16 h) with the CD69 read-out (4
183 h). Here, it seems that a longer activation leads to a stronger signal on immobilized IgG, while
184 shorter activation slightly favours sIC reactivity. FcγRII(R) looked similar to FcγRIIB/C with
185 a slightly higher response to sICs at low stimulant concentrations. Nevertheless, the response
186 to immobilized IgG was higher for both read-outs at higher concentrations. FcγRIIA(H) and
187 FcγRIIIA proved to be the most sensitive towards sICs stimulation. Notably, the reported
188 superior interactivity of sICs with FcγRII (H) over FcγRII (R) (Shashidharamurthy et al, 2009)
189 was not only confirmed using our assay but we also show that this difference is limited to sIC
190 reactivity and is not seen in immobilized IC reactivity (Fig. 2). Additionally, we measured the
191 response of select reporter cell lines towards sICs of different composition (VEGFA/Bvz and
192 IL-5/Mpz). As these sICs incorporate dimeric antigens, we tested if reporter responses were
193 still comparable (Fig. S2). We observed that responses to sICs were generally lower for
194 FcγRIIA(R) but comparable for FcγRI, FcγRIIB/C and FcγRIIIA. Of note, FcγRI showed slight
195 reactivity towards VEGFA/Bvz sICs. Based on the universal transmembrane and cytosolic part
196 of the FcγR chimeras in our assay we concluded that FcγR ectodomains are intrinsically able
197 to differentiate between different conformations of sICs and immobilized monomeric IgG
198 ligands. To validate the data generated by the reporter assay, we determined FcγRIIIA
199 activation using primary human NK cells isolated from PBMCs of three healthy donors. We
200 chose NK cells as they mostly express only one type of FcγR similar to the reporter system and
201 used IL-5/Mpz sICs as NK cells do not respond to IL-5. Measuring a panel of activation markers
202 and cytokine responses by flow cytometry, we observed a differential activation pattern
203 depending on ICs being soluble or immobilized at equal molarity (Fig. 3A). While MIP1-β
204 responses were comparable between the two triggers, degranulation (CD107a) and TNFα

205 responses showed a trend towards lower activation by sICs compared to immobilized IgG
206 (Mpz). Strikingly, IFNγ responses were significantly weaker when NK cells were incubated
207 with sICs compared to immobilized IgG. Next, in order to confirm this to be due to specific
208 activation of FcγRIIIA, we changed the sIC setup by generating reverse-orientation sICs
209 consisting of human FcγR-specific mouse mAbs and goat-anti-mouse IgG $F(ab)_2$ fragments
210 (Fig. S3A). NK cell activation by reverse sICs was compared to NK cell activation by
211 immobilized FcγR specific mAbs. This confirmed our previous observations. As in roughly
212 10% of the population NK cells express FcγRIIC (Anania et al, 2019; Breunis et al, 2008; Lisi
213 et al, 2011; Metes et al, 1998), we also tested reverse sIC activation using an FcγRII specific
214 mAb. As we did not observe an FcγRII-mediated response, we conclude that FcγRIIC
215 expression did not play a role in our experiments (Fig. S3B). Importantly, these experiments
216 validate that all our experimentally synthesized sICs readily activate primary NK cells and
217 induce immunological effector functions.
218 Next, primary neutrophils isolated from whole blood samples of four individual donors were
219 analysed, measuring upregulation of CD11B, CD66B and shedding of L-selectin as markers of
220 immune complex mediated adhesion and activation (Ilton et al, 1999; Khawaja et al, 2019; Lard
221 et al, 1999; Zarbock & Ley, 2009) (Fig. 3B). Again, immobilized IgG and sICs activated
222 primary neutrophils with different efficiency. While both, sICs and immobilized IgG, strongly
223 induced the shedding of L-selectin, the upregulation of CD11B and CD66B showed a tendency
224 towards lower activation by sICs compared to immobilized IgG. As neutrophils express both
225 FcγRIIA and FcγRIIIB, we also individually activated these receptors on neutrophils using
226 immobilized FcγR-specific mAbs. This revealed that neutrophil activation by FcγRs is mostly
227 driven by FcγRIIIB. In light of our previous tests (Fig. 2), this explains the reduced activation
228 by sICs. Taken together, we conclude that primary cells differentiate between opsonized targets
229 and sICs via inherent features of individual FcγRs as well as by the co-expression of FcγRs
230 with different sensitivity towards sICs.

231

232 *Measurement of FcγR activation in response to the molecular size of sICs*

233 We observed that the dimeric CD20:Rtx molecule complex completely failed to trigger FcγR
234 activation (Fig. 1C) while potentially larger sICs, based on multimeric antigens, showed an
235 efficient dose-dependent FcγR activation (Fig. 2, S2). In order to determine whether FcγR
236 signalling responds to changes in sIC size, we cross-titrated amounts of antibody (mAb,
237 infliximab, Ifx) and antigen (Ag, rhTNFα). Specifically, the reporter cells were incubated with
238 sICs of varying mAb:Ag ratio by fixing one parameter and titrating the other. According to the
239 Heidelberger-Kendall precipitation curve (Heidelberger & Kendall, 1929), sIC size depends on
240 the mAb:Ag ratio. sICs of varying sizes result from an excess of either antigen or antibody,
241 leading to the formation of smaller complexes compared to the large molecular complexes
242 formed at around equal molarity. Presumed changes in sIC size were quantified using
243 asymmetrical flow-field flow fractionation (AF4) (Fig. 4A and Table S1). Fig. S4 shows a
244 complete run of an exemplary analysis. Af4 analysis revealed a sIC mean molecular weight of
245 approximately 2130 kDa at a 1:3 ratio (Ifx/TNF-α) with sICs getting smaller with increasing
246 excess of either antigen or antibody, recapitulating a Heidelberger-Kendall-like curve.
247 Incubation of the FcγR reporter cells with sICs of varying size indeed shows that the assay is
248 highly sensitive to changes in sIC size (Fig. 4B). Accordingly, FcγRs showed the strongest
249 responses at mAb:Ag ratios of approximately 1:3. Next, we validated the accuracy of our
250 reporter cell data by subjecting primary human NK cells to the same variation of mAb:Ag
251 stoichiometry. NK cells from three individual donors were measured for MIP1-β upregulation
252 in response to synthetic sICs of varying size and composition (Fig. 4C). Indeed, primary NK
253 cells equally responded to sIC size at the same nanomolar range of stimulating ligand,
254 confirming that the reporter system accurately measures immune cell responses to sICs.
255 Convincingly, NK cell responses to sICs generated from trimeric antigen (TNFα) peaked at a
256 different mAb:Ag ratio compared to NK cell responses to sICs generated from dimeric antigens

257 (IL-5 and VEGFA). TNFα and VEGFA contribute to the activation of resting NK cells, thus
258 leading to higher MIP1-β positivity when NK cells are incubated in the presence of excess
259 antigen. As NK cells do not express IL-5 receptor, this effect is not observed in the presence of
260 excess IL-5. The data reveal a direct correlation between sIC dimension and effector responses.
261 Conversely, when changing antibody concentrations using fixed amounts of antigen, a
262 consistent reduction of NK cell activation is observed in the presence of excess IgG for all three
263 mAb:Ag pairs.
264
265 *Quantification of sIC bioactivity in sera of SLE patients*
266 In order to apply the assay to a clinically relevant setting associated with the occurrence of sICs,
267 we measured circulating sICs present in the serum of SLE patients with varying disease activity.
268 Sera from 4 healthy donors and 25 SLE patients were investigated for FcγRIIIA and FcγRIIB/C
269 activation to compare an activating and an inhibitory receptor. Reporter cells readily secreted
270 mIL-2 in response to patient sera in a dose-dependent manner (Fig. 5A), which was not the case
271 when sera from healthy controls were tested. We confirm that FcγRIIIA and FcγRIIB/C
272 activation depends on the presence of serum sICs by comparing the bioactivity of patient serum
273 before and after polyethylene glycol (PEG) precipitation which is known to deplete sICs (Lux
274 et al, 2013) (Fig. 5B). Next, we calculated the area under the curve (AUC) values for all 25 SLE
275 patient titrations and normalized them to the AUC values measured for healthy individuals. The
276 resulting index values were then correlated with established biomarkers of SLE disease activity,
277 being anti-dsDNA titers (α-dsDNA) and concentrations of the complement cleavage product
278 C3d (Fig. 5C). We observed a significant correlation between our FcγRIIIA activation index
279 values and both disease activity markers ($p=0.0465$ and $p=0.0052$, respectively). FcγRIIB/C
280 activation showed no significant correlation with either biomarker. We assume these
281 interrelations may be due to the influence of IgG sialylation found to be reduced in active SLE
282 (Vuckovic et al, 2015). Generally, de-sialylation of IgG leads to stronger binding by the

activating receptors FcγRI, FcγRIIA and FcγRIII while it reduces the binding affinity of the inhibitory FcγRIIB (Kaneko et al, 2006). In practice, our assay allows the detection and quantification of clinically relevant sICs in sera from SLE patients as shown here or in synovial fluid of rheumatoid arthritis patients (Zhao et al, 2021).

Assay application to in vivo mouse models of lupus and arthritis

BW5147 reporter cells stably expressing chimeric mouse as well as rhesus macaque FcγRs have already been generated using the here described methodology (Kolb et al, 2019; Van den Hoecke et al, 2017). Next we aimed to translate the assay to clinically relevant mouse models. FcγR reporter cells expressing chimeric mouse FcγRs were incubated with sera from lupus (NZB/WF1)(Dubois et al, 1966) or arthritis (K/BxN)(Kouskoff et al, 1996) mice with symptomatic disease. We chose to determine the stimulation of the activating receptors, mFcγRIII and mFcγRIV. Incubation with synthetic sICs generated from rhTNFα and mouse-anti-hTNFα IgG1 showed both of the reporters to be equally responsive to sICs (Fig. 6A). Parental BW5147 cells expressing no FcγRs served as a control. The sera of three mice per group were analysed and compared to sera from wildtype C57BL/6 mice, which served as a healthy control. C57BL/6 mice were chosen, as K/BxN or NZB/WF1 mice show temporal variability in disease onset and presymptomatic phase. We consistently detected mFcγR activation by sera from K/BxN or NZB/WF1 but not healthy C57BL/6 mice (Fig. 6B). While the mFcγRIII responses were generally high and similar between K/BxN and NZB/WF1 mice, mFcγRIV responsiveness tended to be lower and individually more variable. Altogether, the assay enables the reliable detection of sICs in sera of mice with immune-complex mediated diseases making it a promising novel research tool to study the role of sIC formation and FcγR activation in preclinical mouse models.

Discussion

309 In this study we established, validated and applied a new assay system that is able to selectively
310 detect soluble multimeric immune complexes as discrete ligands of FcγRs. Our system is
311 sensitive to the size, concentration and composition of sICs. The assay is scalable and supports
312 measurement with human and mouse FcγRs. It provides two readouts suitable for high-
313 throughput analysis: fast CD69 surface expression and quantifiable IL-2 secretion.
314
315 *A novel assay for the quantification of individual FcγR activation by experimental and clinical*
316 *sICs.*
317 Our methodology provides a comprehensive system, supporting the assessment of essentially
318 all FcγRs, which presents an advantage over previously developed sIC detection and FcγR
319 activation assays (Aoyama et al, 2019; Cheng et al, 2014; Hsieh et al, 2017; Stopforth et al,
320 2018; Szittner et al, 2016; Tada et al, 2014). In contrast to currently available commercial assays
321 detecting sICs by C1q-CIC or C3d ELISA in the micromolar range, our assay measures overall
322 sIC bioactivity in the nanomolar range and has a sole specificity for IgG sICs. The new approach
323 presents with hands on technical advances as it allows for the measurement of small or large
324 amounts of samples by a relatively simple *in vitro* assay with high-throughput potential.
325 Favourably, BW5147 reporter cells are largely inert to human cytokines, which provides a key
326 advantage to measure their responsiveness after contact with human samples. Our pilot study
327 demonstrates that sIC-mediated FcγRIIIA activation correlates with conventional SLE disease
328 markers. This is of great value as a recent analysis shows that circulating sICs and IL-6 can
329 predict SLE activity with the higher accuracy compared to conventional clinical SLE
330 biomarkers (Thanadetsuntorn et al, 2018). However, circulating immune complexes in this
331 study were determined using a commercial C1q-binding ELISA, lacking information on
332 immune cell bioactivity of the measured sICs. Our assay should therefore be explored as an
333 addition to the clinician's toolbox which may allow better disease management. Due to the
334 scalability and high-throughput readouts, the assay can also be of use for larger prospective

335 clinical studies in patients with autoimmune diseases such as SLE or rheumatoid arthritis, where
336 circulating sICs have long been shown to crucially contribute to tissue damage and disease
337 manifestations (Koffler et al, 1971; Levinsky, 1978; Levinsky et al, 1977; Nydegger & Davis,
338 1980; Zubler et al, 1976). Disease-associated, endogenous sICs can also be formed from
339 multimeric viral and bacterial structural proteins generated during infection (Briant et al, 1996;
340 Oh et al, 1992; Vuitton et al, 2020), where circulating sICs strongly impact pathogenesis
341 (Madalinski et al, 1991; Wang & Ravetch, 2015).
342
343 *Dynamic sIC size measurement and monitoring of bioactivity in sIC-associated diseases*
344 The new sIC approach allowed for a simultaneous functional and biophysical assessment of the
345 paradigmatic Heidelberger-Kendall precipitation curve (Heidelberger & Kendall, 1929;
346 Heidelberger & Kendall, 1935). While previous work already revealed that large and small sICs
347 differentially impact IL-6 production in PBMCs (Lux et al, 2013), the dynamics of FcγR
348 activation resulting from constant changes in sIC size have not been explored systematically
349 and lacked resolution of defined FcγR types. We analyzed synthetic sICs formed by highly pure
350 recombinant components via AF4. Our data document that sIC size is indeed governed by
351 antibody:antigen ratios covering a wide range of sizes up to several megadaltons. In the
352 presence of increasing amounts of antibody or antigen deviating from an optimal antibody:ratio,
353 sIC size steadily decreases. Further, by the measurement of FcγR activation we now translate
354 physical sIC size directly to a simple but precise biological read-out. In doing so, we show that
355 sIC size essentially tunes FcγR activation on and off. Thus, our new test system can not only
356 contribute to the functional detection and quantification of clinically relevant sICs but also
357 provides a starting point on how to avoid pathological consequences by influencing the sIC
358 size, for example by administering and monitoring of therapeutic antibodies or recombinant
359 antigens in controlled amounts, thus becoming relevant in clinical pharmacokinetics.
360

361 *Limitations of the reporter system and conclusions*

362 There is a wide range of factors, regulating and influencing the sIC-FcγR interaction. These
363 include Fcγ-FcγR binding affinity and avidity (Koenderman, 2019), IgG subclass, IgG glycan
364 profiles and genetic polymorphism (Bruhns et al, 2009; Pincetic et al, 2014; Plomp et al, 2017;
365 Vidarsson et al, 2014), stoichiometry of antigen-antibody-ratio (Berger et al, 1996; Lux et al,
366 2013; Pierson et al, 2007), FcγR clustering patterns (Patel et al, 2019), downstream signaling
367 (Bournazos et al, 2017; Getahun & Cambier, 2015) and the interaction of FcγR with other
368 receptors (Douek et al, 2009; Ortiz-Stern & Rosales, 2003; Urbaczek et al, 2014; van Egmond
369 et al, 2015; Vanderbruggen et al, 1994). Our assay is sensitive to amount, size and glycosylation
370 of sICs and can readily be adapted to include more FcγR genotypes and polymorphisms by
371 generation of additional reporter cell lines.

372 The major advancements of this reporter system include i) a high accuracy and resolution
373 regarding FcγR type-specific activation compared to traditional indirect assessment via affinity
374 measurements, ii) a scalable and quantifiable assay providing flexible high-throughput readouts
375 in the nanomolar range, iii) an sIC size sensitive reporter system and iv) a comprehensive panel
376 including all human FcγRs. In practice, the platform is suitable to be implemented into small-
377 or large-scale screening setups in research as well as routine laboratories. Prospectively, the
378 reporter cell approach allows for future adaptation as the cells can be equipped with alternative
379 reporter modules to optimize the methodology for specific applications.

380

381 **Materials and Methods**

382

383 *Cell culture:* All cells were cultured in a 5% CO_2 atmosphere at 37°C. BW5147 mouse
384 thymoma cells (BW, kindly provided by Ofer Mandelboim, Hadassah Hospital, Jerusalem,
385 Israel) were maintained at $3x10^5$ to $9x10^5$ cells/ml in Roswell Park Memorial Institute medium
386 (RPMI GlutaMAX, Gibco) supplemented with 10% (vol/vol) fetal calf serum (FCS, Biochrom),

387 sodium pyruvate (1x, Gibco) and β-mercaptoethanol (0.1 mM, Gibco). 293T-CD20 (kindly
388 provided by Irvin Chen, UCLA (Morizono et al, 2010)) were maintained in Dulbecco's
389 modified Eagle's medium (DMEM, Gibco) supplemented with 10% (vol/vol) FCS.
390
391 *BW5147 cell flow cytometry:* BW5147 cells were harvested by centrifugation at 900 g and RT
392 from the suspension culture. $1x10^6$ cells were stained with PE- conjugated anti-human FcγR
393 mAbs (BD) or a PE-TexasRed-conjugated human IgG-Fc fragment (Rockland) for 1h at 4°C in
394 PBS/3%FCS. After 3 washing steps in PBS/3%FCS, the cells were transferred to Flow
395 cytometry tubes (BD) and analysed using BD LSR Fortessa and FlowJo (V10) software. Cells
396 sorting was performed at the Lighthouse core facility of the University Hospital Freiburg using
397 receptor staining (BD Pharmingen, PE-conjugated).
398
399 *Lentiviral transduction:* Lentiviral transduction of BW5147 cells was performed as described
400 previously (Halenius et al, 2011; Kolb et al, 2019; Van den Hoecke et al, 2017). In brief,
401 chimeric FcγR-CD3ζ constructs (Corrales-Aguilar et al, 2013) were cloned into a
402 pUC2CL6IPwo plasmid backbone. For every construct, one 10-cm dish of packaging cell line
403 at roughly 70% density was transfected with the target construct and two supplementing vectors
404 providing the VSV gag/pol and VSV-G-env proteins (6 µg of DNA each) using
405 polyethylenimine (22.5 µg/ml, Sigma) and Polybrene (4 µg/ml; Merck Millipore) in a total
406 volume of 7 ml (2 ml of a 15-min-preincubated transfection mix in serum-free DMEM added
407 to 5 ml of fresh full DMEM). After a medium change, virus supernatant harvested from the
408 packaging cell line 2 days after transfection was then incubated with target BW cells overnight
409 (3.5 ml of supernatant on 10^6 target cells), followed by expansion and pool selection using
410 complete medium supplemented with 2 µg/ml of puromycin (Sigma) over a one week culture
411 period.
412

413 *human IgG suspension ELISA:* 1 µg of IgG1 (rituximab in PBS, 50 µl/well) per well was
414 incubated on a 96well microtiter plate (NUNC Maxisorp) pre-treated (2h at RT) with PBS
415 supplemented with varying percentages (v/v) of FCS (PAN Biotech). IgG1 bound to the plates
416 was detected using an HRP-conjugated mouse-anti-human IgG mAb (Jackson
417 ImmunoResearch).
418
419 *Recombinant antigens and monoclonal antibodies to form sICs:* Recombinant human (rh)
420 cytokines TNF, IL-5, and VEGFA were obtained from Stem Cell technologies. Recombinant
421 CD20 was obtained as a peptide (aa141-188, Acc# P11836) containing the binding region of
422 rituximab (Creative Biolabs). FcγR-specific mAbs were obtained from Stem Cell technologies
423 (CD16: clone 3G8; CD32: IV.3). Reverse sICs were generated from these receptor-specific
424 antibodies using goat-anti-mouse IgG $F(ab)_2$ fragments (Invitrogen) in a 1:1 ratio.
425 Pharmaceutically produced humanized monoclonal IgG1 antibodies infliximab (Ifx),
426 bevacizumab (Bvz), mepolizumab (Mpz) and rituximab (Rtx) were obtained from the
427 University Hospital Pharmacy Freiburg. Mouse anti-hTNFα (IgG2b, R&D Systems, 983003)
428 was used to generate sICs reactive with mouse FcγRs. sICs were generated by incubation of
429 antigens and antibodies in reporter cell medium or PBS for 2 h at 37°C.
430
431 *FcγR receptor activation assay:* FcγR activation was measured adapting a previously described
432 cell-based assay (Corrales-Aguilar et al, 2014; Corrales-Aguilar et al, 2013). The assay was
433 modified to measure FcγR activation in solution. Briefly, $2x10^5$ mouse BW-FcγR (BW5147)
434 reporter cells were incubated with synthetic sICs or diluted serum in a total volume of 100 µl
435 for 16 h at 37°C and 5% CO_2. Incubation was performed in a 96-well ELISA plate (Nunc
436 maxisorp) pre-treated with PBS/10% FCS (v/v) for 1 h at 4°C. Immobilized IgG was incubated
437 in PBS on the plates prior to PBS/10% FCS treatment. After 4h incubation, surface mouse
438 CD69 expression was measured using a high throughout sampler (HTS)-FACS. Reporter cell

439 mouse IL-2 secretion was quantified after 16 h of incubation via anti-IL-2 ELISA as described
440 earlier (Corrales-Aguilar et al, 2013).
441
442 *High throughout sampler flow cytometry (HTS-FACS)*: After 4h of stimulation, $1x10^5$ BW5147
443 reporter cells were stained with APC-conjugated anti-mCD69 (Biolegend; CD69: H1.2F3;
444 1:100) for 30min at 4°C in PBS/3%FCS. Cells were transferred to a U Form 96well Microplate
445 (Greiner 650101) and analysed by flow cytometry (BD Fortessa). High Throughput mode was
446 designed within BD FACSDiva software using HTS mode with the following parameters:
447 sample flow rate 2µl/s, sample volume 10µl, mixing volume 50µl, mixing speed 200µl/s,
448 number of mixes 2 cycles and wash volume 200µl.
449
450 *BW5147 toxicity test:* Cell counting was performed using a Countess II (Life Technologies)
451 according to supplier instructions. Cell toxicity was measured as a ratio between live and dead
452 cells judged by trypan blue staining over a 16 h time frame in a 96well format (100 µl volume
453 per well). BW5147 cells were mixed 1:1 with trypan blue (Invitrogen) and analysed using a
454 Countess II. rhTNFα was diluted in complete medium.
455
456 *NK cell activation flow cytometry:* PBMC were purified from donor blood using Lymphocyte
457 separation Media (Anprotec). Blood draw and PBMC purification from donors was approved
458 by vote 474/18 (ethical review committee, University of Freiburg). Primary NK cells were
459 separated from donor PBMCs via magnetic bead negative selection (Stem Cell technologies)
460 and NK cell purity was confirmed via staining of CD3 (Biolegend, clone HIT3a), CD16
461 (Biolegend, clone 3G8) and CD56 (Miltenyi Biotec, clone AF12-7H3). 96well ELISA plates
462 (Nunc Maxisorp) were pre-treated with PBS/10% FCS (v/v) for 1 h at 4°C. NK cells were
463 stimulated in pre-treated plates and incubated at 37°C and 5% CO_2 for 4 h. Golgi Plug and
464 Golgi Stop solutions (BD) were added as suggested by supplier. CD107a (APC, BD, H4A3)

465 specific conjugated mAb was added at the beginning of the incubation period. Following the
466 stimulation period, MIP-1β (PE, BD Pharmingen), IFNγ (BV-510, Biolegends, 4SB3) and
467 TNFα (PE/Cy7, Biolegends, MAB11) production was measured via intracellular staining
468 Cytokines (BD, CytoFix/CytoPerm, Kit as suggested by the supplier). 50 ng/ml PMA
469 (InvivoGen) + 0.5 µM Ionomycin (InvivoGen) were used as a positive stimulation control for
470 NK cell activation. After 3 washing steps in PBS/3%FCS, the cells were transferred to Flow
471 cytometry tubes (BD) and analysed using a BD FACS Fortessa and FlowJo (V10) software.
472
473 *Neutrophil adhesion and activation flow cytometry*: Human primary neutrophil granulocytes
474 were isolated from whole blood of healthy donors via magnetic bead negative selection
475 (Stemcell #19666). 96well ELISA plates (Nunc Maxisorp) were pre-treated with PBS/10% FCS
476 (v/v) for 1 h at 4°C. Per reaction, $2x10^5$ cells/ml neutrophils were stimulated with ICs in Roswell
477 Park Memorial Institute medium (RPMI GlutaMAX, Gibco) supplemented with 10% (vol/vol)
478 fetal calf serum (FCS, Biochrom) and incubated at 37°C and 5% CO_2 for 30 min. Adhesion and
479 activation markers of neutrophils were measured by surface staining of CD11B (APC,
480 Biolegend, ICRF44), CD66B (FITC, Stemcell, G10F5) and L-selectin (PE, Biolegend, DREG-
481 56)(Ilton et al, 1999; Khawaja et al, 2019; Lard et al, 1999; Veen et al, 1998). Cells were then
482 analysed by flow cytometry. FcγRII or FcγRIII cross-linking controls were performed by
483 immobilization of receptor specific mAbs (Stem cell technologies, IV.3 and 3G8) before the
484 ELISA plate was blocked.
485
486 *Asymmetric flow field flow fractionation (AF4):* The AF4 system consisted of a flow controller
487 (Eclipse AF4, Wyatt), a MALS detector (DAWN Heleos II, Wyatt), a UV detector (1260
488 Infinity G1314F, Agilent) and the separation channel (SC channel, PES membrane, cut-off 10
489 kDa, 490 µm spacer, wide type, Wyatt). Elution buffer: 1.15 g/L Na_2HPO_4 (Merck), 0.20 g/L
490 NaH_2PO_4 x H_2O (Merck), 8.00 g/L NaCl (Sigma) and 0,20 g/L NaN_3 (Sigma), adjusted to pH

491 7.4, filtered through 0.1 µm. AF4 sequence (Vx = cross flow in mL/min): (a) elution (2 min,
492 Vx: 1.0); (b) focus (1 min, Vx: 1.0), focus + inject (1 min, Vx: 1.0, inject flow: 0.2 mL/min),
493 repeated three times; (c) elution (30 min, linear Vx gradient: 1.0 to 0.0); (d) elution (15 min,
494 Vx: 0.0); (e) elution + inject (5 min, Vx: 0.0). A total protein mass of 17±0.3 µg (Ifx, rhTNFα
495 or ICs, respectively) was injected. The eluted sample concentration was calculated from the UV
496 signal at 280 nm using extinction coefficients of 1.240 mL/(mg cm) or 1.450 mL/(mg cm) in
497 the case of TNFα or Ifx, respectively. For the ICs, extinction coefficients were not available
498 and difficult to calculate as the exact stoichiometry is not known. An extinction coefficient of
499 1.450 mL/(mg cm) was used for calculating the molar masses of all ICs. Especially in the case
500 of ICs rich in TNFα, the true coefficients should be lower, and the molar masses of these
501 complexes are overestimated by not more than 14 %. The determined molar masses for TNFα-
502 rich complexes are therefore biased but the observed variations in molar mass for the different
503 ICs remain valid. The mass-weighted mean of the distribution of molar masses for each sample
504 was calculated using the ASTRA 7 software package (Wyatt).
505
506 *SLE patient cohort:* Sera from patients with SLE were obtained from the Immunologic,
507 Rheumatologic Biobank (IR-B) of the Department of Rheumatology and Clinical Immunology.
508 Biobanking and the project were approved by the local ethical committee of the University of
509 Freiburg (votes 507/16 and 624/14). All patients who provided blood to the biobank had
510 provided written informed consent. Ethical Statement: The study was designed in accordance
511 with the guidelines of the Declaration of Helsinki (revised 2013). Patients with SLE (n = 25)
512 and healthy controls (n = 4) were examined. All patients met the revised ACR classification
513 criteria for SLE. Disease activity was assessed using the SLEDAI-2K score. C3d levels were
514 analyzed in EDTA plasma using rocket double decker immune-electrophoresis with antisera
515 against C3d (Polyclonal Rabbit Anti-Human C3d Complement, Agilent) and C3c (Polyclonal
516 Rabbit Anti-Human C3c Complement Agilent) as previously described (Rother et al, 1993).

517 Anti-human dsDNA antibodies titers were determined in serum using an anti-dsDNA IgG
518 ELISA kit (diagnostik-a GmbH).
519
520 *Patient serum IC precipitation:* For polyethylene glycol (PEG) precipitation human sera were
521 mixed with PEG 6000 (Sigma-Aldrich) in PBS at a final concentration of 10% PEG 6000. After
522 overnight incubation at 4°C, ICs were precipitated by centrifugation at 2000 x g for 30 min at
523 4 °C, pellets were washed once with PEG 6000 and then centrifuged at 2000 x g for 20 min at
524 4 °C. Supernatants were harvested and precipitates re-suspended in pre-warmed PBS for 1 h at
525 37 °C. IgG concentrations of serum, precipitates and supernatants obtained after precipitation
526 were quantified by Nanodrop (Thermo Scientific™) measurement.
527
528 *Mice and Models:* Animal experiments were approved by the local governmental commission
529 for animal protection of Freiburg (Regierungspräsidium Freiburg, approval no. G16/59 and
530 G19/21). Lupus-prone (NZBxNZW)F1 mice (NZB/WF1) were generated by crossing
531 NZB/BlNJ mice with NZW/LacJ mice, purchased from The Jackson Laboratory. KRNtg mice
532 were obtained from F. Nimmerjahn (Universität Erlangen-Nürnberg) with the permission of D.
533 Mathis and C. Benoist (Harvard Medical School, Boston, MA), C57BL/6 mice (BL/6) and
534 NOD/ShiLtJArc (NOD/Lt) mice were obtained from the Charles River Laboratories. K/BxN
535 (KRNtgxNOD)F1 mice (K/BxN) were obtained by crossing KRNtg mice and NOD/Lt mice.
536 All mice were housed in a 12-h light/dark cycle, with food and water ad libitum. Mice were
537 euthanized and blood collected for serum preparation from 16 weeks old BL/6 animals, from
538 16 weeks old arthritic K/BxN animals and from 26 – 38 weeks old NZB/WF1 mice with
539 established glomerulonephritis.
540
541 *Statistical analyses:* Statistical analyses were performed using Graphpad Prism software (v6)
542 and appropriate tests.

543

544 **Supplementary Materials**

545 Fig. S1. rhTNFα is not toxic to mouse lymphocyte BW5147 cells even at high concentrations.

546 Fig. S2. FcγRs are activated by VEGFA and IL-5 sICs

547 Fig. S3. Distinct activation patterns of NK cells incubated with inverse sICs

548 Fig. S4. AF4 elution profiles of Ifx/TNFα-immune complexes.

549 Table S1. Analysis of the molar mass distribution of ICs from AF4 data.

550

551 **Figure legends**

552

553 **Fig. 1. Establishment of a cell-based reporter assay measuring FcγR activation in response**
554 **to sICs.** A) BW5147 reporter cells stably expressing human FcγR-ζ chain chimeras or BW5147
555 parental cells (grey/dashed) were stained with FcγR specific conjugated mAbs as indicated and
556 measured for surface expression of FcγRs via flow cytometry. B) FCS coating of an ELISA
557 microtiter plate allows for suspension of subsequently added IgG. Plate bound IgG was
558 quantified via ELISA. C) Immobilized IC, immobilized IgG and IgG opsonized cells represent
559 qualitatively similar ligands for FcγRs. Response curves of human FcγRs activated by
560 opsonized cells (293T cells stably expressing CD20 + Rituximab [Rtx]), immobilized IC (rec.
561 soluble CD20 + Rtx) and immobilized IgG (Rtx). sICs formed using monovalent antigen (rec.
562 soluble CD20 + Rtx) do not activate human FcγRs. X-Axis shows sample concentration
563 determined by antibody molarity. Y-Axis shows FcγR activation determined by reporter cell
564 mouse IL-2 production (OD 450nm). Two independent experiments performed in technical
565 duplicates. Error bars = SD. D) Schematic of used assay setups. BW5147 reporter cells
566 expressing chimeric human FcγR receptors express endogenous CD69 or secrete mouse IL-2
567 in response to FcγR activation by clustered IgG. sICs are generated using mAbs and multivalent
568 antigens. sIC suspension requires pre-blocking of an ELISA plate using PBS supplemented
569 with 10% FCS (FCS coat, grey-dashed).

570

571 **Fig. 2. FcγRs are activated by sICs formed from multivalent antigens.** Ultra-pure antigen
572 (Ag, TNF-α) mixed with therapy-grade mAb (infliximab, Ifx) was used to generate sICs. X-
573 Axis: concentrations of stimulant expressed as molarity of either mAb or Ag monomer and IC
574 (expressed as mAb molarity) at a mAb:Ag ratio of 1:2. Soluble antigen or soluble antibody
575 alone served as negative controls and were not sufficient to activate human FcγRs. Immobilized
576 IgG (Rtx) or immobilized FcγR-specific mAbs served as positive controls. Two independent

577 experiments performed in technical duplicates. Error bars = SD. Error bars smaller than
578 symbols are not shown. Left panel: IL-2 quantification 16 h after reporter cell activation.
579 Background (blank) was subtracted (dashed line). IL-2 was measured via anti-IL-2 ELISA
580 (A_{450nm}) and IL-2 concentrations were calculated from an IL-2 standard. Right panel: Reporter
581 cell CD69 expression 4 h post trigger was measured using flow cytometry. MFI were
582 normalized to untreated cells (ctrl.) and are presented as fold-change increase.
583
584 **Fig. 3. The FcγR-dependent activation pattern of primary NK cells or primary**
585 **neutrophils depends on IC solubility**. A) Negatively selected primary NK cells purified from
586 PBMCs of three healthy donors were tested for activation markers using flow cytometry. NK
587 cells were incubated with immobilized IgG (mepolizumab, Mpz), soluble IC (Mpz:IL-5 = 1:1),
588 soluble Mpz or soluble IL-5 (all at 200 nM, 10^6 cells). Incubation with PMA and Ionomycin
589 (Iono) served as a positive control. Incubation with medium alone served as a negative control.
590 Means of technical duplicates. Error bars = SD. One-way ANOVA (Tukey); *p<0.05,
591 **p<0.01, ***p<0.001, ****p<0.0001. B) Negatively selected primary neutrophils purified
592 from whole blood of four healthy donors were tested for adhesion and activation markers using
593 flow cytometry. Neutrophils were incubated with immobilized IgG (Mpz), soluble IC (Mpz:IL-
594 5 = 1:1), soluble Mpz or soluble IL-5 (all at 200 nM, $2*10^5$ cells). Incubation with PMA or
595 immobilized rituximab served as positive controls. Incubation with medium served as a
596 negative control. Immobilized FcγRII and FcγRIII specific mAbs served as functional controls.
597 Mean florescence intensity (MFI) values at t=30 minutes of incubation are presented as increase
598 over t=0 min. Means of technical duplicates. Error bars = SD. Two-way ANOVA compared to
599 medium (Dunnett); *p<0.05, **p<0.01, ***p<0.001, ****p<0.0001.
600
601 **Fig. 4. FcγRIIB/C and FcγR-IIIA respond to sIC size reproducing a Heidelberger-Kendall**
602 **like precipitation curve.** A) infliximab (mAb) and rhTNFα (Ag) were mixed at different ratios

603 (17 µg total protein, calculated from monomer molarity) and analysed via AF4. sIC size is
604 maximal at a 1:3 ratio of mAb:Ag and reduced when either mAb or Ag are given in excess.
605 $\langle M \rangle_w$ = mass-weighted mean of the molar mass distribution. Three independent experiments.
606 Error bars = SD. Data taken from Table S1. One complete run analysis is shown in Fig. S2. B)
607 sICs of different size were generated by cross-titration according to the AF4 determination.
608 Reporter cells were incubated with fixed amounts of either mAb (infliximab, left) or Ag
609 (rhTNFα, right) and titrated amounts of antigen or antibody, respectively. X-Axis shows
610 titration of either antigen or antibody, respectively (TNFα calculated as monomer). Two
611 independent experiments performed in technical duplicates. Error bars = SD. C) Purified
612 primary NK cells from three different donors were incubated with cross-titrated sICs as in A.
613 NK cells were measured for MIP-1β expression (% positivity). Incubation with PMA and
614 Ionomycin served as a positive control. Incubation with medium alone served as a negative
615 control. Measured in technical duplicates. Error bars = SD.
616
617 **Fig. 5. The reporter assay enables quantification of serum-derived sICs from SLE**
618 **patients.** Serum derived sIC from systemic lupus erythematosus (SLE) patients activate human
619 FcγR reporter cells. 25 patients and 4 healthy control individuals were separated into three
620 groups for measurement. A) Experiments shown for an exemplary group of 8 SLE patients and
621 two healthy individuals. Dose-dependent reactivity of FcγRs IIIA and IIB/C was observed only
622 for SLE patient sera and not for sera from healthy individuals. One exemplary experiment
623 performed in technical duplicates. Error bars = SD. B) Activation of FcγRs IIB/C and IIIA by
624 patient serum is mediated by serum derived sICs. Patient serum samples were depleted of sICs
625 by PEG precipitation and the supernatant (SN) was compared to untreated serum regarding
626 FcγR activation (left). One experiment performed in technical duplicates. Error bars =SD. IgG
627 concentration in the precipitate (PC), supernatant (SN) or unfractionated serum respectively is
628 shown in the bar graph (right). C) FcγR activation data from A was compared to conventional

629 SLE disease markers (α-dsDNA levels indicated as IU/ml or C3d concentrations indicated as
630 mg/L). FcγR activation from a dose-response curve as in A was calculated as area under curve
631 (AUC) for each SLE patient (n=25) or healthy individual (n=4) and expressed as fold change
632 compared to the healthy control mean. SLE patients with α-dsDNA levels below 50 IU/ml and
633 C3d values below 6 mg/L were excluded. One-tailed Spearman's.
634
635 **Fig. 6. The reporter assay can be applied to mouse models of autoimmune disease.** A)
636 Reporter cells expressing mFcγRIII, mFcγRIV or parental BW5147 cells were incubated with
637 titrated amounts of synthetic sICs generated from rhTNFα and mouse-anti-hTNFα at a 1:1 ratio
638 by mass. One experiment performed in technical duplicates. Error bars = SD. B) Titrations of
639 3 mouse sera per group (C57BL/6, K/BxN or NZB/WF1) were incubated with mFcγR reporter
640 cells and FcγR activation was assessed as described above. Sera from BL/6 mice served as
641 negative control. Two independent experiments in technical duplicates. Error bars = SD.
642
643
644
645
646
647
648
649
650
651
652
653
654

References

Anania JC, Chenoweth AM, Wines BD, Hogarth PM (2019) The Human FcgammaRII (CD32) Family of Leukocyte FcR in Health and Disease. Front Immunol 10: 464

Antes U, Heinz HP, Schultz D, Brackertz D, Loos M (1991) C1q-bearing immune complexes detected by a monoclonal antibody to human C1q in rheumatoid arthritis sera and synovial fluids. Rheumatol Int 10: 245-250

Aoyama M, Tada M, Ishii-Watabe A (2019) A Cell-Based Reporter Assay Measuring the Activation of Fc Gamma Receptors Induced by Therapeutic Monoclonal Antibodies. Methods Mol Biol 1904: 423-429

Bano A, Pera A, Almoukayed A, Clarke THS, Kirmani S, Davies KA, Kern F (2019) CD28 (null) CD4 T-cell expansions in autoimmune disease suggest a link with cytomegalovirus infection. F1000Res 8

Berger S, Ballo H, Stutte HJ (1996) Immune complex-induced interleukin-6, interleukin-10 and prostaglandin secretion by human monocytes: A network of pro- and anti-inflammatory cytokines dependent on the antigen:antibody ratio. Eur J Immunol 26: 1297-1301

Bohm S, Kao D, Nimmerjahn F (2014) Sweet and sour: the role of glycosylation for the anti-inflammatory activity of immunoglobulin G. Current topics in microbiology and immunology 382: 393-417

Bournazos S, Wang TT, Dahan R, Maamary J, Ravetch JV (2017) Signaling by Antibodies: Recent Progress. Annu Rev Immunol 35: 285-311

Breunis WB, van Mirre E, Bruin M, Geissler J, de Boer M, Peters M, Roos D, de Haas M, Koene HR, Kuijpers TW (2008) Copy number variation of the activating FCGR2C gene predisposes to idiopathic thrombocytopenic purpura. Blood 111: 1029-1038

Briant L, Coudronniere N, Robert-Hebmann V, Benkirane M, Devaux C (1996) Binding of HIV-1 virions or gp120-anti-gp120 immune complexes to HIV-1-infected quiescent peripheral blood mononuclear cells reveals latent infection. J Immunol 156: 3994-4004

Bruhns P (2012) Properties of mouse and human IgG receptors and their contribution to disease models. Blood 119: 5640-5649

Bruhns P, Iannascoli B, England P, Mancardi DA, Fernandez N, Jorieux S, Daeron M (2009) Specificity and affinity of human Fcgamma receptors and their polymorphic variants for human IgG subclasses. Blood 113: 3716-3725

Bruhns P, Jonsson F (2015) Mouse and human FcR effector functions. Immunol Rev 268: 25-51

Chauhan AK (2017) Editorial: Immune Complexes in Disease Pathology. Front Immunol 8: 173

Cheng ZJ, Garvin D, Paguio A, Moravec R, Engel L, Fan F, Surowy T (2014) Development of a robust reporter-based ADCC assay with frozen, thaw-and-use cells to measure Fc effector function of therapeutic antibodies. J Immunol Methods 414: 69-81

Corrales-Aguilar E, Trilling M, Hunold K, Fiedler M, Le VT, Reinhard H, Ehrhardt K, Merce-Maldonado E, Aliyev E, Zimmermann A et al (2014) Human cytomegalovirus Fcgamma binding

proteins gp34 and gp68 antagonize Fcgamma receptors I, II and III. PLoS pathogens 10: e1004131

Corrales-Aguilar E, Trilling M, Reinhard H, Merce-Maldonado E, Widera M, Schaal H, Zimmermann A, Mandelboim O, Hengel H (2013) A novel assay for detecting virus-specific antibodies triggering activation of Fcgamma receptors. Journal of immunological methods 387: 21-35

Douek DC, Rittirsch D, Flierl MA, Day DE, Nadeau BA, Zetoune FS, Sarma JV, Werner CM, Wanner GA, Simmen H-P et al (2009) Cross-Talk between TLR4 and FcγReceptorIII (CD16) Pathways. Plos Pathog 5: e1000464

Dubois EL, Horowitz RE, Demopoulos HB, Teplitz R (1966) NZB/NZW mice as a model of systemic lupus erythematosus. JAMA 195: 285-289

Duchemin AM, Ernst LK, Anderson CL (1994) Clustering of the High-Affinity Fc Receptor for Immunoglobulin-G (Fc-Gamma-Ri) Results in Phosphorylation of Its Associated Gamma-Chain. J Biol Chem 269: 12111-12117

Fossati G, Bucknall RC, Edwards SW (2002) Insoluble and soluble immune complexes activate neutrophils by distinct activation mechanisms: changes in functional responses induced by priming with cytokines. Ann Rheum Dis 61: 13-19

Getahun A, Cambier JC (2015) Of ITIMs, ITAMs, and ITAMis: revisiting immunoglobulin Fc receptor signaling. Immunol Rev 268: 66-73

Granger V, Peyneau M, Chollet-Martin S, de Chaisemartin L (2019) Neutrophil Extracellular Traps in Autoimmunity and Allergy: Immune Complexes at Work. Front Immunol 10: 2824

Greenberg S, Chang P, Silverstein SC (1994) Tyrosine phosphorylation of the gamma subunit of Fc gamma receptors, p72syk, and paxillin during Fc receptor-mediated phagocytosis in macrophages. J Biol Chem 269: 3897-3902

Halenius A, Hauka S, Dolken L, Stindt J, Reinhard H, Wiek C, Hanenberg H, Koszinowski UH, Momburg F, Hengel H (2011) Human cytomegalovirus disrupts the major histocompatibility complex class I peptide-loading complex and inhibits tapasin gene transcription. J Virol 85: 3473-3485

Heidelberger M, Kendall FE (1929) A Quantitative Study of the Precipitin Reaction between Type Iii Pneumococcus Polysaccharide and Purified Homologous Antibody. J Exp Med 50: 809-823

Heidelberger M, Kendall FE (1935) The Precipitin Reaction between Type Iii Pneumococcus Polysaccharide and Homologous Antibody : Iii. A Quantitative Study and a Theory of the Reaction Mechanism. J Exp Med 61: 563-591

Hsieh YT, Aggarwal P, Cirelli D, Gu L, Surowy T, Mozier NM (2017) Characterization of Fc gamma RIIIA effector cells used in in vitro ADCC bioassay: Comparison of primary NK cells with engineered NK-92 and Jurkat T cells. Journal of Immunological Methods 441: 56-66

Ilton MK, Langton PE, Taylor ML, Misso NL, Newman M, Thompson PJ, Hung J (1999) Differential expression of neutrophil adhesion molecules during coronary artery surgery with cardiopulmonary bypass. J Thorac Cardiovasc Surg 118: 930-937

Kaneko Y, Nimmerjahn F, Ravetch JV (2006) Anti-inflammatory activity of immunoglobulin G resulting from Fc sialylation. Science 313: 670-673

765
766 Khawaja AA, Pericleous C, Ripoll VM, Porter JC, Giles IP (2019) Autoimmune rheumatic
767 disease IgG has differential effects upon neutrophil integrin activation that is modulated by the
768 endothelium. Sci Rep 9: 1283
769
770 Kiefer F, Brumell J, Al-Alawi N, Latour S, Cheng A, Veillette A, Grinstein S, Pawson T (1998)
771 The Syk protein tyrosine kinase is essential for Fc gamma receptor signaling in macrophages
772 and neutrophils. Mol Cell Biol 18: 4209-4220
773
774 Koenderman L (2019) Inside-Out Control of Fc-Receptors. Front Immunol 10: 544
775
776 Koffler D, Agnello V, Thoburn R, Kunkel HG (1971) Systemic lupus erythematosus: prototype
777 of immune complex nephritis in man. J Exp Med 134: 169-179
778
779 Kolb P, Hoffmann K, Sievert A, Reinhard H, Merce-Maldonado E, Le-Trilling VTK, Halenius A,
780 Gutle D, Hengel H (2021) Human Cytomegalovirus antagonizes activation of Fcgamma
781 receptors by distinct and synergizing modes of IgG manipulation. Elife 10
782
783 Kolb P, Sijmons S, McArdle MR, Taher H, Womack J, Hughes C, Ventura A, Jarvis MA, Stahl-
784 Hennig C, Hansen S et al (2019) Identification and Functional Characterization of a Novel Fc
785 Gamma-Binding Glycoprotein in Rhesus Cytomegalovirus. J Virol 93
786
787 Kouskoff V, Korganow AS, Duchatelle V, Degott C, Benoist C, Mathis D (1996) Organ-specific
788 disease provoked by systemic autoimmunity. Cell 87: 811-822
789
790 Lagasse HAD, Hengel H, Golding B, Sauna ZE (2019) Fc-Fusion Drugs Have FcgammaR/C1q
791 Binding and Signaling Properties That May Affect Their Immunogenicity. AAPS J 21: 62
792
793 Lard LR, Mul FPJ, de Haas M, Roos D, Duits AJ (1999) Neutrophil activation in sickle cell
794 disease. J Leukocyte Biol 66: 411-415
795
796 Levinsky RJ (1978) Role of circulating soluble immune complexes in disease. Arch Dis Child
797 53: 96-99
798
799 Levinsky RJ, Cameron JS, Soothill JF (1977) Serum immune complexes and disease activity
800 in lupus nephritis. Lancet 1: 564-567
801
802 Lisi S, Sisto M, Lofrumento DD, D'Amore S, D'Amore M (2011) Advances in the understanding
803 of the Fc gamma receptors-mediated autoantibodies uptake. Clin Exp Med 11: 1-10
804
805 Lu LL, Suscovich TJ, Fortune SM, Alter G (2018) Beyond binding: antibody effector functions
806 in infectious diseases. Nat Rev Immunol 18: 46-61
807
808 Luo Y, Pollard JW, Casadevall A (2010) Fcgamma receptor cross-linking stimulates cell
809 proliferation of macrophages via the ERK pathway. J Biol Chem 285: 4232-4242
810
811 Lux A, Yu X, Scanlan CN, Nimmerjahn F (2013) Impact of immune complex size and
812 glycosylation on IgG binding to human FcgammaRs. J Immunol 190: 4315-4323
813
814 Madalinski K, Burczynska B, Heermann KH, Uy A, Gerlich WH (1991) Analysis of viral proteins
815 in circulating immune complexes from chronic carriers of hepatitis B virus. Clin Exp Immunol
816 84: 493-500
817
818 Mayadas TN, Tsokos GC, Tsuboi N (2009) Mechanisms of immune complex-mediated
819 neutrophil recruitment and tissue injury. Circulation 120: 2012-2024
820

821 Metes D, Ernst LK, Chambers WH, Sulica A, Herberman RB, Morel PA (1998) Expression of
822 functional CD32 molecules on human NK cells is determined by an allelic polymorphism of the
823 FcgammaRIIC gene. Blood 91: 2369-2380
824
825 Morizono K, Ku A, Xie Y, Harui A, Kung SK, Roth MD, Lee B, Chen IS (2010) Redirecting
826 lentiviral vectors pseudotyped with Sindbis virus-derived envelope proteins to DC-SIGN by
827 modification of N-linked glycans of envelope proteins. J Virol 84: 6923-6934
828
829 Mulligan MS, Hevel JM, Marletta MA, Ward PA (1991) Tissue-Injury Caused by Deposition of
830 Immune-Complexes Is L-Arginine Dependent. P Natl Acad Sci USA 88: 6338-6342
831
832 Nimmerjahn F, Ravetch JV (2006) Fcgamma receptors: old friends and new family members.
833 Immunity 24: 19-28
834
835 Nimmerjahn F, Ravetch JV (2008) Fcgamma receptors as regulators of immune responses.
836 Nat Rev Immunol 8: 34-47
837
838 Nimmerjahn F, Ravetch JV (2010) Antibody-mediated modulation of immune responses.
839 Immunol Rev 236: 265-275
840
841 Nydegger UE, Davis JSt (1980) Soluble immune complexes in human disease. CRC Crit Rev
842 Clin Lab Sci 12: 123-170
843
844 Oh SK, Cruikshank WW, Raina J, Blanchard GC, Adler WH, Walker J, Kornfeld H (1992)
845 Identification of HIV-1 envelope glycoprotein in the serum of AIDS and ARC patients. J Acquir
846 Immune Defic Syndr (1988) 5: 251-256
847
848 Ortiz-Stern A, Rosales C (2003) Cross-talk between Fc receptors and integrins. Immunol Lett
849 90: 137-143
850
851 Patel KR, Roberts JT, Barb AW (2019) Multiple Variables at the Leukocyte Cell Surface Impact
852 Fc gamma Receptor-Dependent Mechanisms. Front Immunol 10: 223
853
854 Pierson TC, Xu Q, Nelson S, Oliphant T, Nybakken GE, Fremont DH, Diamond MS (2007) The
855 stoichiometry of antibody-mediated neutralization and enhancement of West Nile virus
856 infection. Cell Host Microbe 1: 135-145
857
858 Pincetic A, Bournazos S, DiLillo DJ, Maamary J, Wang TT, Dahan R, Fiebiger BM, Ravetch
859 JV (2014) Type I and type II Fc receptors regulate innate and adaptive immunity. Nat Immunol
860 15: 707-716
861
862 Plomp R, Ruhaak LR, Uh HW, Reiding KR, Selman M, Houwing-Duistermaat JJ, Slagboom
863 PE, Beekman M, Wuhrer M (2017) Subclass-specific IgG glycosylation is associated with
864 markers of inflammation and metabolic health. Sci Rep 7: 12325
865
866 Rajan TV (2003) The Gell-Coombs classification of hypersensitivity reactions: a re-
867 interpretation. Trends in immunology 24: 376-379
868
869 Rother E, Lang B, Coldewey R, Hartung K, Peter HH (1993) Complement split product C3d as
870 an indicator of disease activity in systemic lupus erythematosus. Clin Rheumatol 12: 31-35
871
872 Shashidharamurthy R, Zhang F, Amano A, Kamat A, Panchanathan R, Ezekwudo D, Zhu C,
873 Selvaraj P (2009) Dynamics of the interaction of human IgG subtype immune complexes with
874 cells expressing R and H allelic forms of a low-affinity Fc gamma receptor CD32A. J Immunol
875 183: 8216-8224
876

Stopforth RJ, Oldham RJ, Tutt AL, Duriez P, Chan HTC, Binkowski BF, Zimprich C, Li D, Hargreaves PG, Cong M et al (2018) Detection of Experimental and Clinical Immune Complexes by Measuring SHIP-1 Recruitment to the Inhibitory FcgammaRIIB. J Immunol 200: 1937-1950

Szittner Z, Bentlage AEH, Rovero P, Migliorini P, Lorand V, Prechl J, Vidarsson G (2016) Label-free detection of immune complexes with myeloid cells. Clin Exp Immunol 185: 72-80

Tada M, Ishii-Watabe A, Suzuki T, Kawasaki N (2014) Development of a cell-based assay measuring the activation of FcgammaRIIa for the characterization of therapeutic monoclonal antibodies. Plos One 9: e95787

Tahir S, Fukushima Y, Sakamoto K, Sato K, Fujita H, Inoue J, Uede T, Hamazaki Y, Hattori M, Minato N (2015) A CD153+CD4+ T follicular cell population with cell-senescence features plays a crucial role in lupus pathogenesis via osteopontin production. J Immunol 194: 5725-5735

Tanaka M, Krutzik SR, Sieling PA, Lee DJ, Rea TH, Modlin RL (2009) Activation of Fc gamma RI on monocytes triggers differentiation into immature dendritic cells that induce autoreactive T cell responses. J Immunol 183: 2349-2355

Thanadetsuntorn C, Ngamjanyaporn P, Setthaudom C, Hodge K, Saengpiya N, Pisitkun P (2018) The model of circulating immune complexes and interleukin-6 improves the prediction of disease activity in systemic lupus erythematosus. Sci Rep 8: 2620

Urbaczek AC, Toller-Kawahisa JE, Fonseca LM, Costa PI, Faria CM, Azzolini AE, Lucisano-Valim YM, Marzocchi-Machado CM (2014) Influence of FcgammaRIIIb polymorphism on its ability to cooperate with FcgammaRIIa and CR3 in mediating the oxidative burst of human neutrophils. Hum Immunol 75: 785-790

Van den Hoecke S, Ehrhardt K, Kolpe A, El Bakkouri K, Deng L, Grootaert H, Schoonooghe S, Smet A, Bentahir M, Roose K et al (2017) Hierarchical and Redundant Roles of Activating FcgammaRs in Protection against Influenza Disease by M2e-Specific IgG1 and IgG2a Antibodies. J Virol 91

van Egmond M, Vidarsson G, Bakema JE (2015) Cross-talk between pathogen recognizing Toll-like receptors and immunoglobulin Fc receptors in immunity. Immunol Rev 268: 311-327

Vanderbruggen T, Kok PTM, Raaijmakers JAM, Lammers JWJ, Koenderman L (1994) Cooperation between Fc-Gamma Receptor-Ii and Complement Receptor-Type-3 during Activation of Platelet-Activating-Factor Release by Cytokine-Primed Human Eosinophils. Journal of Immunology 153: 2729-2735

Veen JCCMI, Grootendorst DC, Bel EH, Smits HH, van der Keur M, Sterk PJ, Hiemstra PS (1998) CD11b and L-selectin expression on eosinophils and neutrophils in blood and induced sputum of patients with asthma compared with normal subjects. Clinical and Experimental Allergy 28: 606-615

Vidarsson G, Dekkers G, Rispens T (2014) IgG subclasses and allotypes: from structure to effector functions. Front Immunol 5: 520

Vossebeld PJ, Homburg CH, Roos D, Verhoeven AJ (1997) The anti-Fc gamma RIII mAb 3G8 induces neutrophil activation via a cooperative actin of Fc gamma RIIIb and Fc gamma RIIa. Int J Biochem Cell Biol 29: 465-473

Vuckovic F, Kristic J, Gudelj I, Teruel M, Keser T, Pezer M, Pucic-Bakovic M, Stambuk J, Trbojevic-Akmacic I, Barrios C et al (2015) Association of systemic lupus erythematosus with decreased immunosuppressive potential of the IgG glycome. Arthritis Rheumatol 67**:** 2978-2989

Vuitton DA, Vuitton L, Seilles E, Galanaud P (2020) A plea for the pathogenic role of immune complexes in severe Covid-19. Clin Immunol 217**:** 108493

Wang TT, Ravetch JV (2015) Immune complexes: not just an innocent bystander in chronic viral infection. Immunity 42**:** 213-215

Ward PA, Fattahi F, Bosmann M (2016) New Insights into Molecular Mechanisms of Immune Complex-Induced Injury in Lung. Front Immunol 7**:** 86

Yamada DH, Elsaesser H, Lux A, Timmerman JM, Morrison SL, de la Torre JC, Nimmerjahn F, Brooks DG (2015) Suppression of Fcgamma-receptor-mediated antibody effector function during persistent viral infection. Immunity 42**:** 379-390

Zarbock A, Ley K (2009) Neutrophil adhesion and activation under flow. Microcirculation 16**:** 31-42

Zhao S, Grieshaber-Bouyer R, Rao DA, Kolb P, Chen H, Andreeva I, Tretter T, Lorenz HM, Watzl C, Wabnitz G et al (2021) JAK inhibition prevents the induction of pro-inflammatory HLA-DR(+) CD90(+) RA synovial fibroblasts by IFN. Arthritis Rheumatol

Zubler RH, Nydegger U, Perrin LH, Fehr K, McCormick J, Lambert PH, Miescher PA (1976) Circulating and intra-articular immune complexes in patients with rheumatoid arthritis. Correlation of 125I-Clq binding activity with clinical and biological features of the disease. J Clin Invest 57**:** 1308-1319

964 **Acknowledgements:** We thank T. Schleyer (IR-B Biobank) for providing patient samples. We
965 are indebted to Falk Nimmerjahn (Universität Erlangen-Nürnberg) for providing KRNtg mice.
966 **Funding:** This work was supported by an intramural junior investigator fund of the Faculty of
967 Medicine to PK (EQUIP - Funding for Medical Scientists, Faculty of Medicine, University of
968 Freiburg), by the German Research foundation (DFG) (FOR2830 HE 2526/9-1) to HH, by the
969 DFG research grant TRR130 to REV and the Ministry of Science, Research, and Arts Baden-
970 Württemberg (Margarete von Wrangell Programm) to NC. **Competing interests:** The authors
971 declare no financial and non-financial competing interests. **Data and materials availability:**
972 All data associated with this study are present in the paper or Supplementary Materials.
973

974 **Author contribution**

975 Conceived and designed the experiments: P.K., H.C., A.M-P., M.H.
976 Performed the experiments: P.K., H.C., M.H., A.M-P, U.S.
977 Analyzed the data: P.K., H.C., A.M-P, U.S.
978 Contributed/reagent/sample material: RE.V.
979 Writing and original draft preparation: P.K., H.C.
980 Review and editing: H.H., RE.V., P.K.
981

982 **Figures**

983

984 **Figure 1**

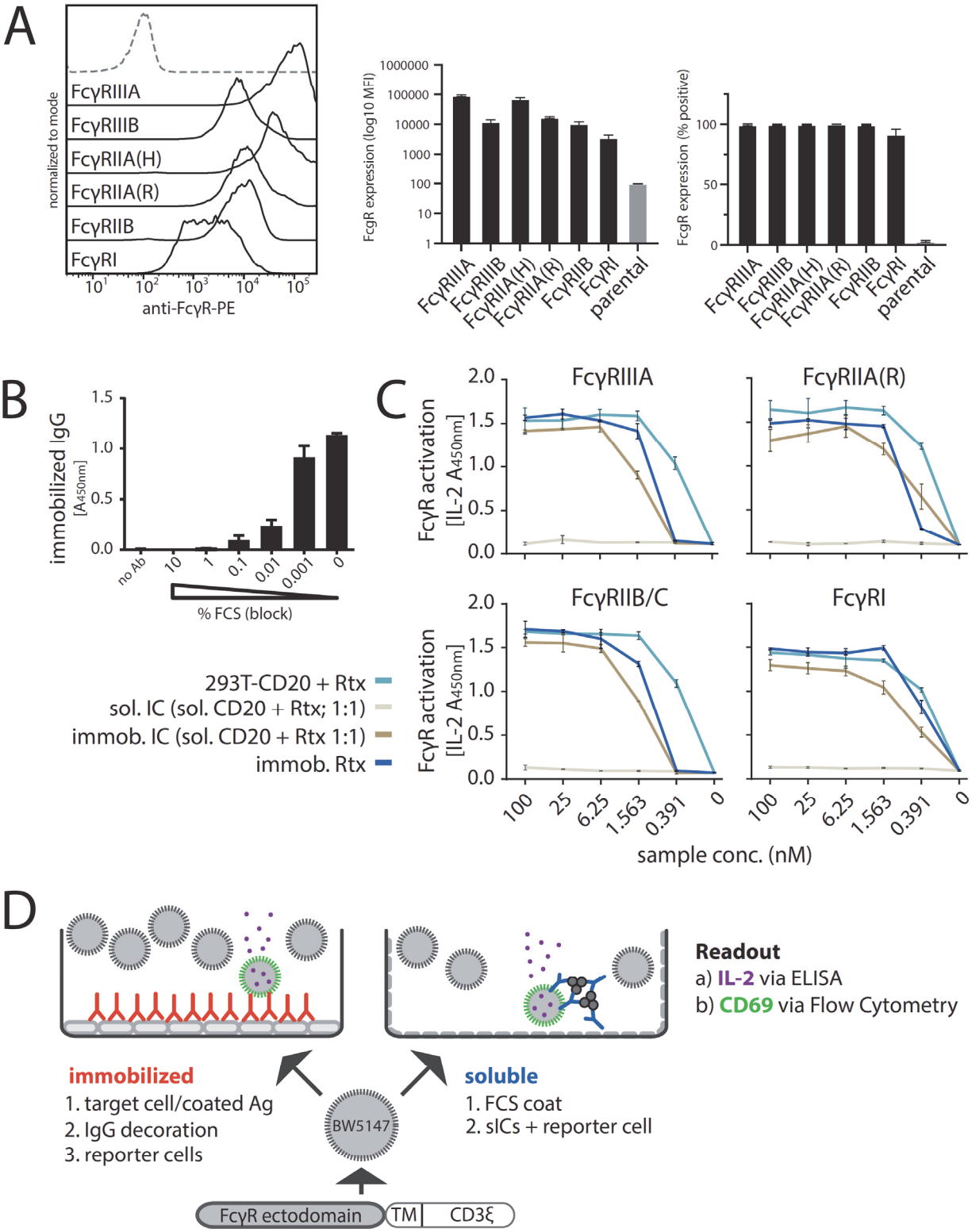

985

986

987 **Figure 2**

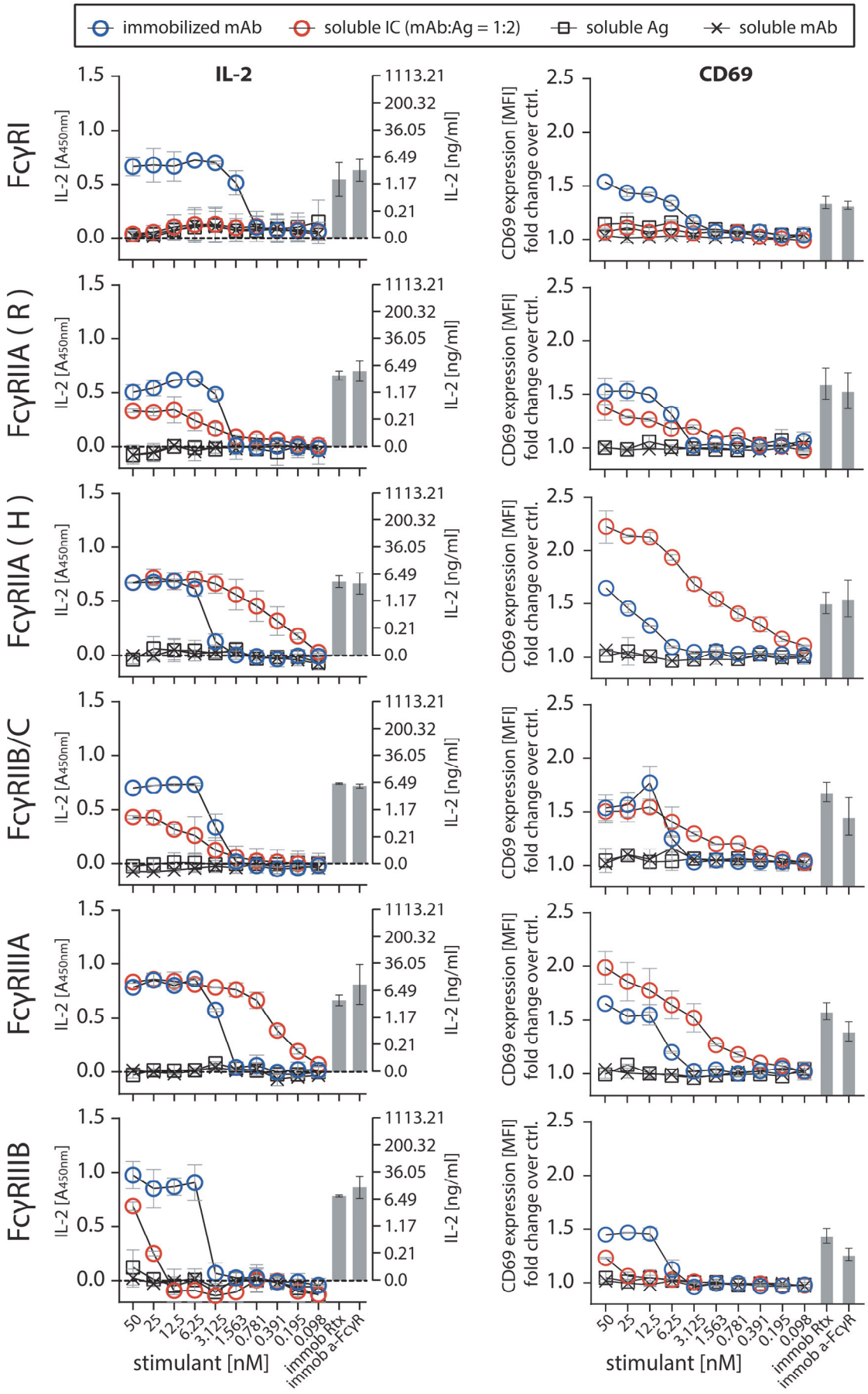

988

989 **Figure 3**

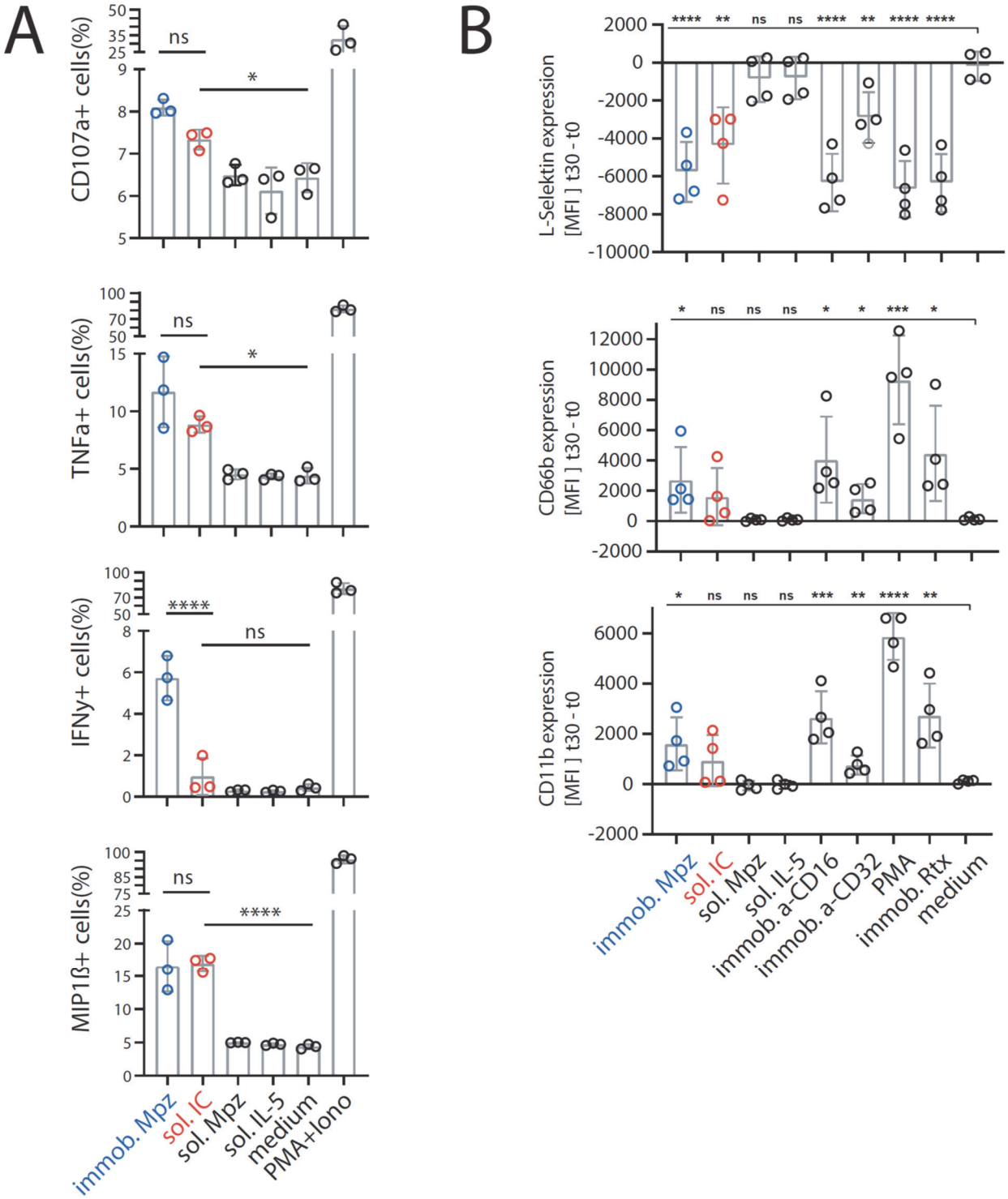

990

991

992

993 **Figure 4**

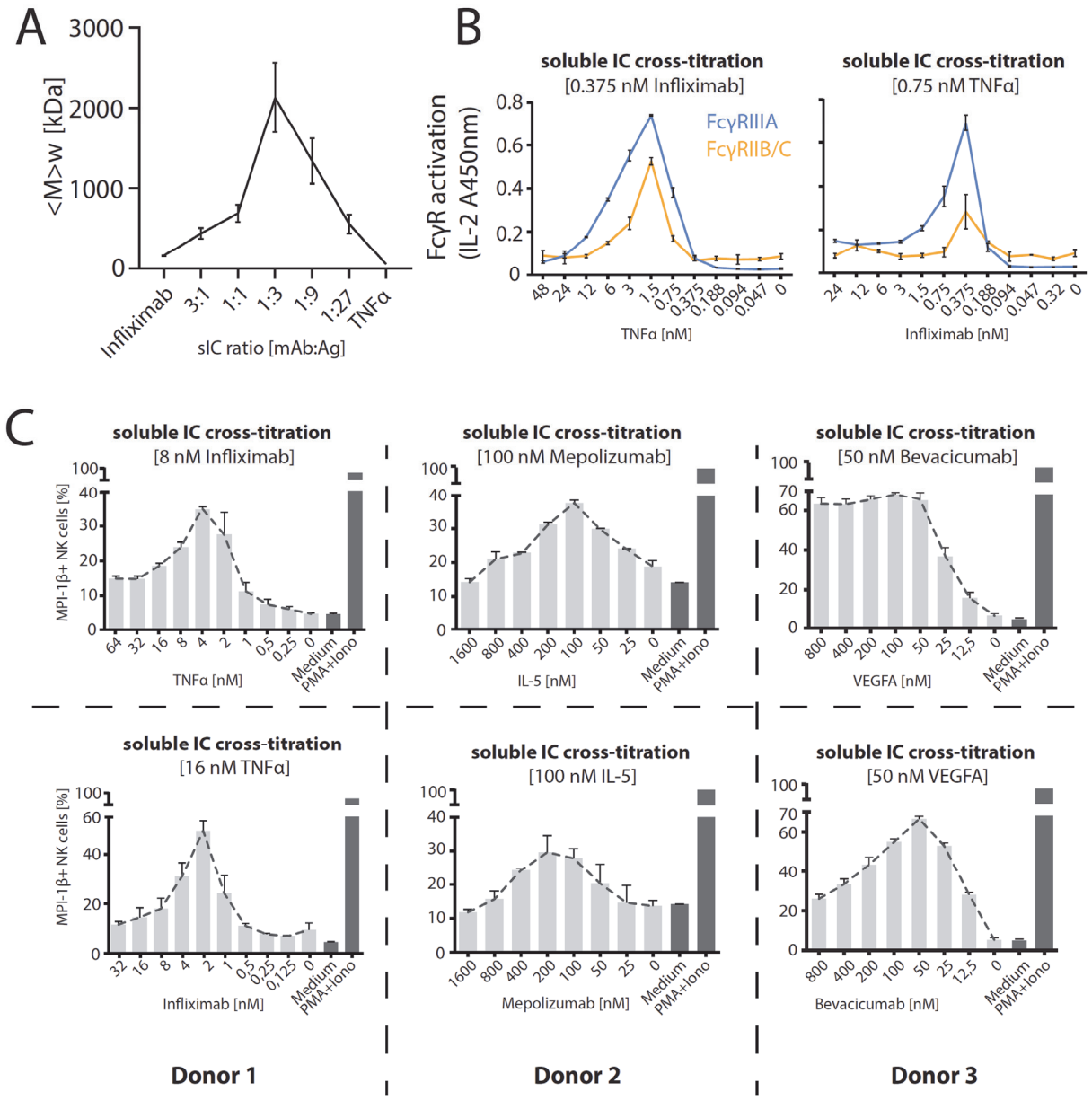

994

995

996

997 **Figure 5**

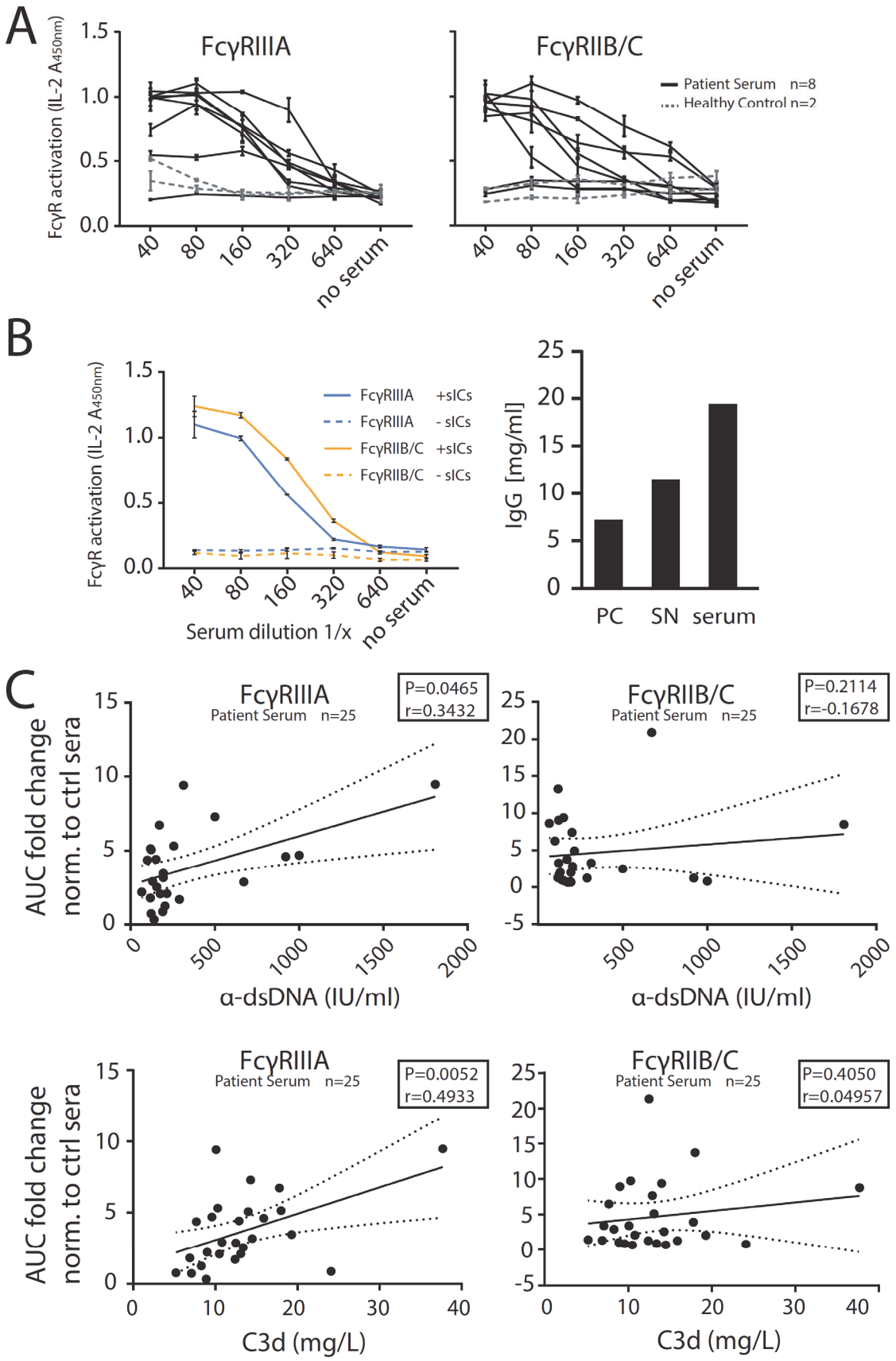

998

999 **Figure 6**

1000

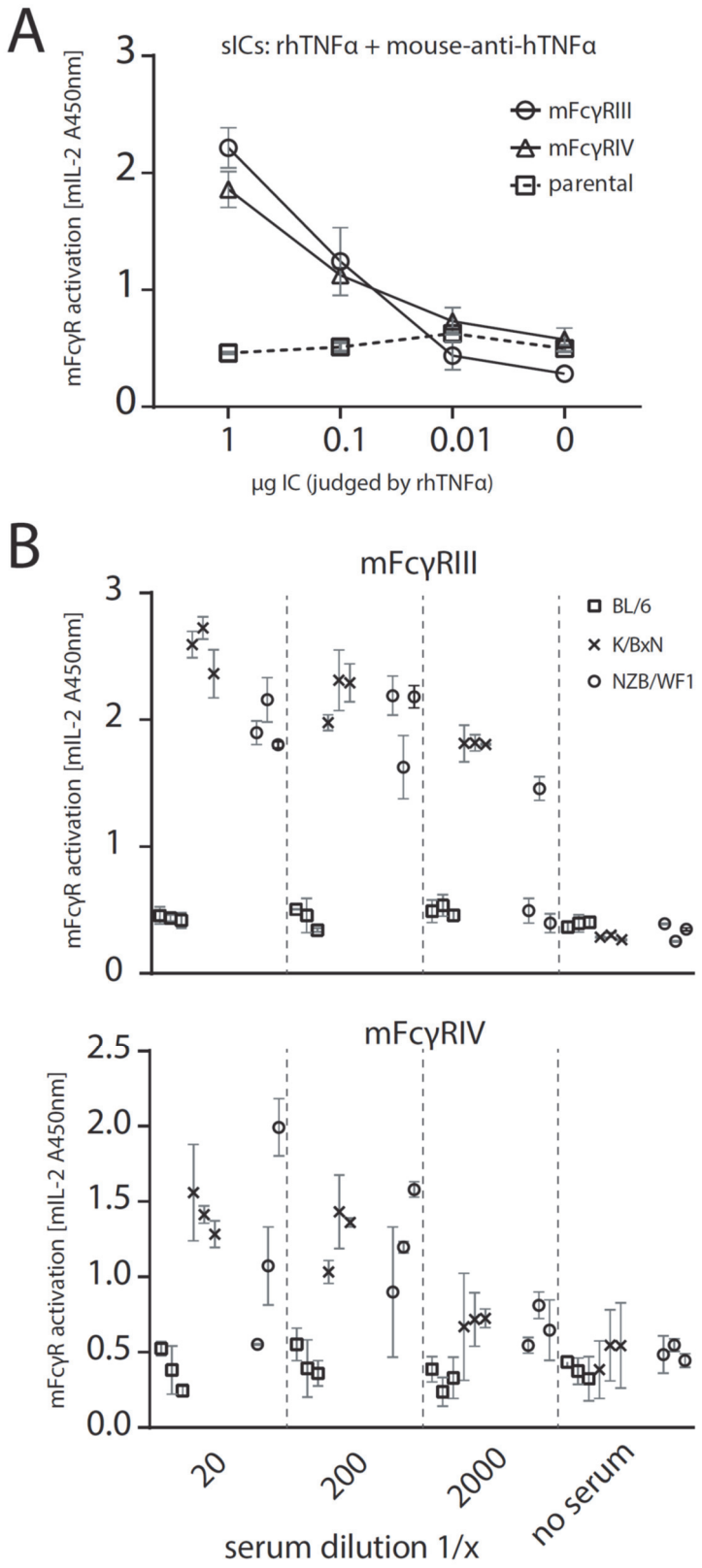

1001

1002

1003

1004 **Supplementary material**

1005

1006 **Figure S1**

1007

1008

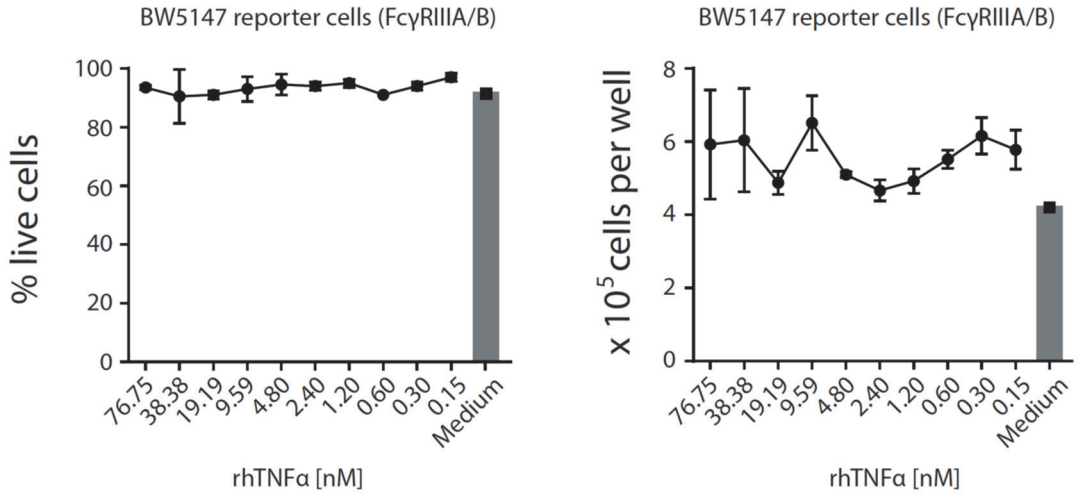

1009

1010 **Fig. S1. rhTNFα is not toxic to mouse lymphocyte BW5147 cells even at high**
1011 **concentrations**. Cell count and percentage of live cells were unaltered over a 16 h time frame
1012 of reporter cell culture in the presence of indicated rhTNFα concentrations and comparable to
1013 regular growth in complete medium. Experiments were conducted in 3 replicates. Error bars =
1014 SD.

1015

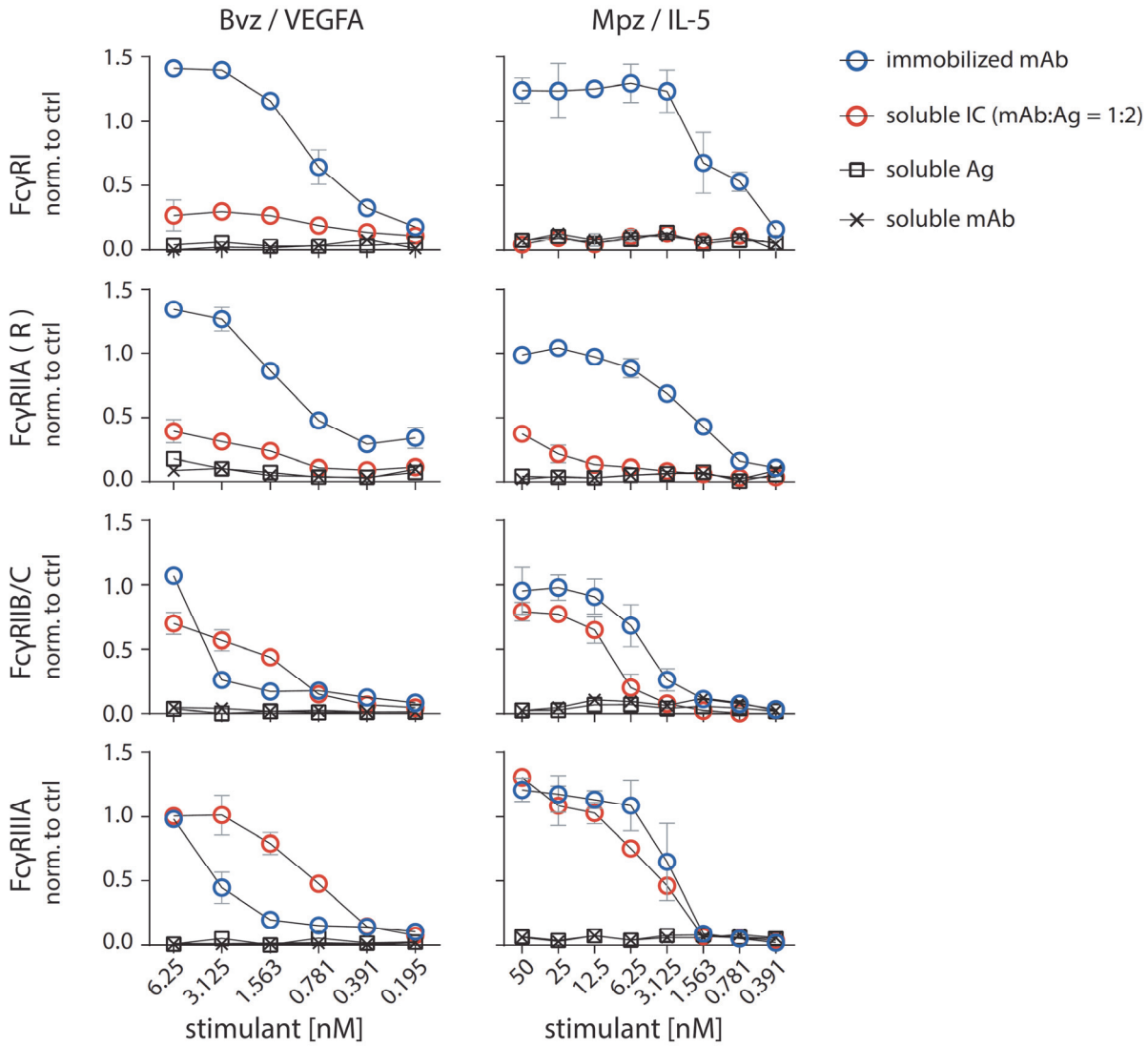

Fig. S2. FcγRs are activated by sICs formed from multivalent antigens. Two different multivalent ultra-pure antigens (Ag) mixed with respective therapy-grade mAbs were used to generate sICs as indicated for each set of graphs (top to bottom). IC pairs: mepolizumab (Mpz) and rhIL-5; bevacizumab (Bvz) and rhVEGFA. X-Axis: concentrations of stimulant expressed as molarity of either mAb or Ag monomer and IC (expressed as mAb molarity) at a mAb:Ag ratio of 1:2. Soluble antigen or soluble antibody alone served as negative controls and were not sufficient to activate human FcγRs. FcγR responses were normalized to immobilized rituximab (Rtx) at 1 µg/well (set to 1) and a medium control (set to 0). Two independent experiments performed in technical duplicates. Error bars = SD. Error bars smaller than symbols are not shown.

1027

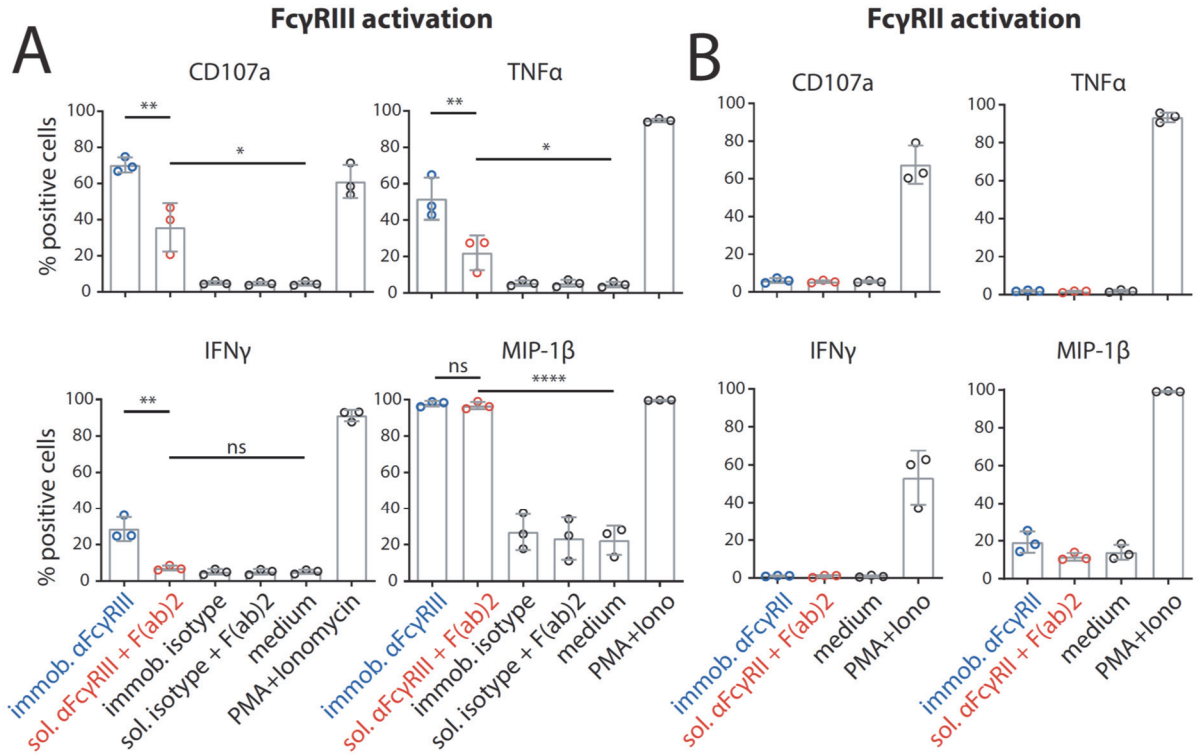

1028

1029 **Fig. S3. Distinct activation patterns of NK cells incubated with inverse sICs.** Negatively
1030 selected primary NK cells purified from PBMCs of three healthy donors were tested for NK
1031 cell activation markers. Error bars = SD. One-way ANOVA (Tukey); *p<0.05, **p<0.01,
1032 ***p<0.001, ****p<0.0001. A) NK cells were incubated for 4 h with immobilized FcγRIII-
1033 specific mAb, soluble mouse-anti-human IgG $F(ab)_2$ complexed FcγRIII-specific mAb (reverse
1034 sICs), immobilized IgG of non-FcγRIII-specificity (isotype control) or soluble $F(ab)_2$
1035 complexed isotype control (all at 1µg, 10^6 cells). Incubation with PMA and Ionomycin served
1036 as a positive control. Incubation with medium alone served as a negative control. B) As in A
1037 using an FcγRII-specific mAb. NK cells from the tested donors in this study do not react to
1038 FcγRII activation.

1039 **Figure S4**

1040

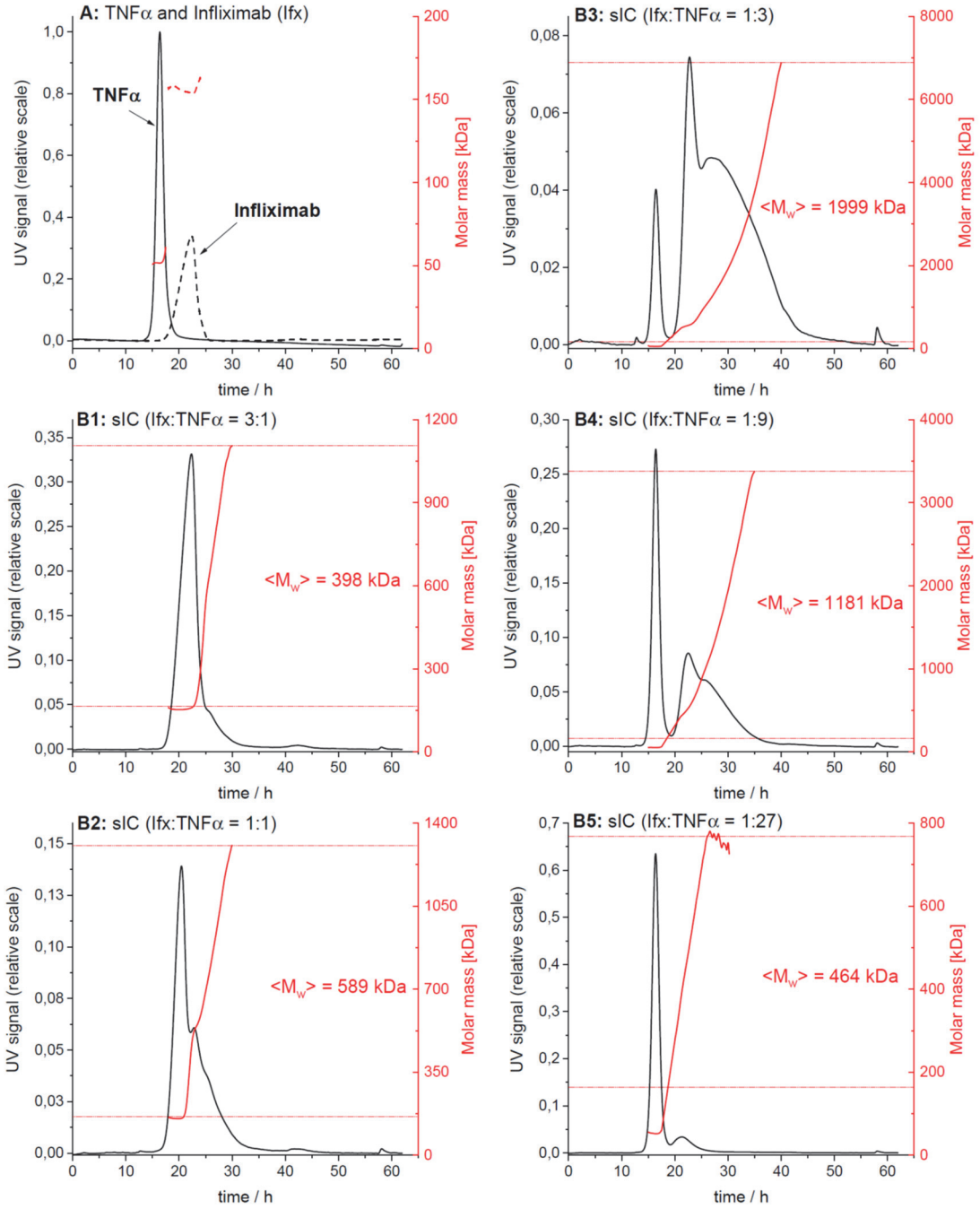

1041

1042

1043 **Fig. S4. AF4 elution profiles of Ifx/TNFα-immune complexes.**

1044 The elution profiles from one of three independent runs are shown. Protein concentration in the
1045 eluate is shown in black (UV signal at λ = 280 nm, normalized to the highest UV signal found
1046 in this experiment), molar masses determined by MALS for a given retention time in red.
1047 Horizontal red lines indicate the range of molar masses used to calculate the mass-weighted
1048 mean of molar masses $<M_w>$. A) Overlay of the elution profiles obtained for TNFα and Ifx,
1049 respectively; B1 to B5) Elution profiles for sICs formed after incubation of TNFα and Ifx at
1050 different molar ratios.

1051

1052 **Table S1**

Sample	Range of assigned molar masses [kDa]			Mass-weighted mean of assigned molar masses [kDa]			
	Run 1	Run 2	Run 3	Run 1	Run 2	Run 3	Mean ± SD
Infliximab, IFX	158 – 182	153 – 164	159 – 193	162	156	163	160 ± 4
TNF -alpha	52 – 55	51 – 61	52 – 62	52	52	52	52 ± 0
Immune complexes							
IFX/TNF 3:1	182 – $1.16 \cdot 10^3$	164 – $1.11 \cdot 10^3$	193 – $1.10 \cdot 10^3$	409	398	518	442 ± 66
IFX/TNF 1:1	182 – $2.06 \cdot 10^3$	164 – $1.31 \cdot 10^3$	193 – $1.42 \cdot 10^3$	801	589	681	690 ± 106
IFX/TNF 1:3	182 – $5.05 \cdot 10^3$	164 – $6.89 \cdot 10^3$	193 – $10.8 \cdot 10^3$	$1.77 \cdot 10^3$	$2.00 \cdot 10^3$	$2.61 \cdot 10^3$	$2.13 \cdot 10^3$ ± 435
IFX/TNF 1:9	182 – $5.36 \cdot 10^3$	164 – $3.38 \cdot 10^3$	193 – $3.51 \cdot 10^3$	$1.66 \cdot 10^3$	$1.18 \cdot 10^3$	$1.17 \cdot 10^3$	$1.34 \cdot 10^3$ ± 279
IFX/TNF 1:27	182 – $1.68 \cdot 10^3$	164 – 768	193 – $1.01 \cdot 10^3$	689	464	521	558 ± 117

1053

1054 **Table S1. Analysis of the molar mass distribution of ICs from AF4 data.**

1055 For a given elution time, the AF4 profiles provide the concentration (UV) at which a given
1056 molar mass (MALS) of a protein is present in the sample. The molar mass distribution of Ifx,
1057 TNFα and their immune complexes (sICs) was obtained by plotting the cumulative frequency
1058 as a function of molar mass. For a selected range of molar masses, a mass-weighted mean value
1059 ($<M_w>$) was calculated. All detected molar masses were selected in the case of Ifx and TNFα
1060 whereas only molar masses larger than the maximal molar mass found for Ifx were assigned to
1061 sICs. The table shows the range of assigned molar masses and the calculated $<M_w>$ for each
1062 AF4 run (n = 3).